agammaglobulinemia compared with healthy children, Pediatr. Res. 51 (2002) 159–168.
[4] D. Vetrie, I. Vorechovsky, P. Sideras, et al., The gene involved in X-linked agammaglobulinemia is a member of the *src* family of protein-tyrosine kinases, Nature 361 (1993) 226–233.
[5] S. Tsukada, D.C. Saffran, D.J. Rawlings, et al., Deficient expression of a B cell cytoplasmic tyrosine kinase in human X-linked agammaglobulinemia, Cell 72 (1993) 279–290.
[6] J. Väliaho, C.I. Smith, M. Vihinen, BTKbase: the mutation database for X-linked agammaglobulinemia, Hum. Mutat. 27 (2006) 1209–1217.
[7] T. Futatani, T. Miyawaki, S. Tsukada, et al., Deficient expression of Bruton's tyrosine kinase in monocytes from X-linked agammaglobulinemia as evaluated by a flow cytometric analysis and its clinical application to carrier detection, Blood 91 (1998) 595–602.
[8] M. Yamada, T. Ariga, N. Kawamura, et al., Determination of carrier status for the Wiskott–Aldrich syndrome by flow cytometric analysis of Wiskott–Aldrich syndrome protein expression in peripheral blood mononuclear cells, J. Immunol. 165 (2000) 1119–1122.
[9] S. Hashimoto, S. Tsukada, M. Matsushita, et al., Identification of Bruton's tyrosine kinase (Btk) gene mutations and characterization of the derived proteins in 35 X-linked agammaglobulinemia families: a nationwide study of Btk deficiency in Japan, Blood 88 (1996) 561–573.
[10] I. Vorechovský, M. Vihinen, G. de Saint Basile, et al., DNA-based mutation analysis of Bruton's tyrosine kinase gene in patients with X-linked agammaglobulinaemia, Hum. Mol. Genet. 4 (1995) 51–58.
[11] D.M. Stewart, C.C. Kurman, D.L. Nelson, Production of monoclonal antibodies to Bruton's tyrosine kinase, Hybridoma 14 (1995) 243–246.
[12] H.B. Gaspar, L.A. Bradley, F. Katz, et al., Mutation analysis in Bruton's tyrosine kinase, the X-linked agammaglobulinemia gene, including identification of an insertional hotspot, Hum. Mol. Genet. 4 (1995) 755–757.
[13] H. Jin, A.D. Webster, M. Vihinen, et al., Identification of Btk mutations in 20 unrelated patients with X-linked agammaglobulinaemia (XLA), Hum. Mol. Genet. 4 (1995) 693–700.
[14] E. Holinski-Feder, M. Weiss, O. Brandau, et al., Mutation screening of the BTK gene in 56 families with X-linked agammaglobulinemia (XLA): 47 unique mutations without correlation to clinical course, Pediatrics 101 (1998) 276–284.
[15] S. Kobayashi, T. Iwata, M. Saito, et al., Mutations of the Btk gene in 12 unrelated families with X-linked agammaglobulinemia in Japan, Hum. Genet. 97 (1996) 424–430.
[16] H. Kaneko, N. Kawamoto, T. Asano, et al., Leaky phenotype of X-linked agammaglobulinaemia in a Japanese family, Clin. Exp. Immunol. 140 (2005) 520–523.
[17] J.G. Noordzij, S. de Bruin-Versteeg, N.G. Hartwig, et al., XLA patients with BTK splice-site mutations produce low levels of wild-type BTK transcripts, J. Clin. Immunol. 22 (2002) 306–318.
[18] D.M. Stewart, L. Tian, D.L. Nelson, A case of X-linked agammaglobulinemia diagnosed in adulthood, Clin. Immunol. 99 (2001) 94–99.
[19] S. Nonoyama, S. Tsukada, T. Yamadori, et al., Functional analysis of peripheral blood B cells in patients with X-linked agammaglobulinemia, J. Immunol. 161 (1998) 3925–3929.
[20] A. Broides, W. Yang, M.E. Conley, Genotype/phenotype correlations in X-linked agammaglobulinemia, Clin. Immunol. 118 (2006) 195–200.
[21] E. López-Granados, R. Pérez de Diego, A. Ferreira Cerdán, et al., A genotype–phenotype correlation study in a group of 54 patients with X-linked agammaglobulinemia, J. Allergy Clin. Immunol. 116 (2005) 690–697.

Please cite this article as: K. Maekawa, et al., X-linked agammaglobulinemia in a 10-year-old boy with a novel non-invariant splice-site mutation in *Btk* gene, Blood Cells Mol. Diseases (2010), doi:10.1016/j.bcmd.2010.01.004

Pediatr Blood Cancer 2010;54:329–331

BRIEF REPORT

Successful Treatment of Refractory Donor Lymphocyte Infusion-Induced Immune-Mediated Pancytopenia with Rituximab

Itaru Kato, MD,[1] Katsutsugu Umeda, MD,[1]* Tomonari Awaya, MD,[1] Yoshihiro Yui, MD,[1] Akira Niwa, MD,[1] Hisanori Fujino, MD,[1] Hiroshi Matsubara, MD,[1] Ken-Ichiro Watanabe, MD,[1] Toshio Heike, MD,[1] Naoto Adachi, MD,[2] Fumio Endo, MD,[2] Tomoyuki Mizukami, MD,[3] Hiroyuki Nunoi, MD,[3] Tatsutoshi Nakahata, MD,[1] and Souichi Adachi, MD[1]

A 6-year-old male with chronic granulomatous disease, who was transplanted with bone marrow and exhibited increasing mixed chimerism, subsequently received two donor lymphocyte infusions (DLI). Two weeks after the second DLI, the patient developed acute graft-versus-host disease (GVHD) and progressive pancytopenia that was associated with autoantibody production. Conventional treatment did not improve the pancytopenia. However, administration of Rituximab (RTX) (375 mg/m^2/week for four consecutive weeks) resulted in a rapid resolution of the pancytopenia. The patient achieved full donor chimerism without GVHD symptoms. RTX can be valuable for managing immune-mediated cytopenias that arise after DLI and are refractory to conventional therapies. Pediatr Blood Cancer 2010;54:329–331. © 2009 Wiley-Liss, Inc.

Key words: allogeneic stem cell transplantation; antibodies; graft rejection; graft-versus-host disease; immune responses; Rituximab

INTRODUCTION

Donor leukocyte infusion (DLI) is used as an immunotherapy not only for preventing the reemergence of malignancies, but also for preventing graft rejection after allogeneic hematopoietic stem cell transplantation (hSCT) that results in the development of mixed increasing chimerism [1]. However, DLI treatment is also associated with substantial toxicity. For example, it has been shown that up to 41% of patients receiving DLI suffer from myelosuppression, which could lead to death from causes other than the underlying disease [2,3]. Like the cytopenias associated with graft-versus-host disease (GVHD), the cytopenias that can arise after DLI are conventionally treated by steroids, intravenous immunoglobulin (IVIG), and splenectomy. However, the prognosis of cases that are refractory to conventional treatments remains dismal as the treatment of such cases has not been established. Anti-CD20 antibody (Rituximab, RTX), a humanized murine monoclonal antibody that is often used to treat B-cell malignancies, has been shown to effectively treat various autoimmune diseases that arise after hSCT [4–6]. Here, we describe a patient with severe immune-mediated pancytopenia after DLI who responded well to RTX therapy.

CASE REPORT

A 4-month-old male was diagnosed with X-linked chronic granulomatous disease on the basis of his reduced NADPH oxidase levels (<5%) and the complete absence of gp91-phox. Despite prophylactic treatment with trimethoprim–sulfamethoxazole and itraconazole, and interferon-γ, he suffered repeatedly from severe bacterial and fungal infections, including multiple episodes of pulmonary aspergillosis. Therefore, allogeneic hSCT was planned, and the patient was transferred at 6 years of age to our hospital for bone marrow transplantation (BMT) from a genotypically HLA-matched, blood-type compatible unrelated donor. The HLA type of the donor and the patient was HLA-A 33/24, -B 58/52, -DR 1302/1502. The conditioning regimen included fludarabine 30 mg/m^2/day for 6 days from day −7 to −2, cyclophosphamide 30 mg/kg/day for 4 days from day −6 to −3, anti-T lymphocyte globulin 2.5 mg/kg/day for 4 days from day −6 to −3, and total body irradiation 300 cGy on day −1. To prevent GVHD, the patient received tacrolimus and short-methotrexate (day 1: 10 mg/m^2, day 3.6: 7 mg/m^2), as previously reported [7]. Subsequently, 4.8×10^8/kg mononucleated cells were infused without T-cell depletion. The patient's bone marrow (BM) was analyzed serially for chimerism by microsatellite PCR, and the presence of oxidase-positive neutrophils in the peripheral blood (PB) was determined by fluorescence-activated cell sorting using a dihydrorhodamine oxidation assay. Hematopoietic engraftment occurred rapidly. The neutrophil count exceeded 0.5×10^9/L on day 10, the reticulocyte count exceeded 10‰ on day 17, and the platelet counts did not drop below 40×10^9/L during this period. However, the donor chimerism of the patient was unstable. After the dosage of tacrolimus was reduced on day 25, grade II acute GVHD of the skin developed on day 37, which was resolved by a short course of prednisolone (PSL) treatment. Subsequently, the patient achieved full donor chimerism of BM on day 61, and the oxidase-positivity of PB neutrophils was 100% on day 82. The GVHD did not worsen after treatment with PSL and tacrolimus was discontinued on days 98 and 361, respectively.

Although the patient was asymptomatic and there were no abnormal laboratory findings, the oxidase-positivity of PB neutrophils gradually decreased to 50% and 13% on days 404 and 758,

[1]Department of Pediatrics, Graduate School of Medicine, Kyoto University, Kyoto, Japan; [2]Department of Pediatrics, Graduate School of Medicine, Kumamoto University, Kumamoto, Japan; [3]Faculty of Medicine, Department of Pediatrics, University of Miyazaki, Miyazaki, Japan

The authors declare no competing financial interests.

*Correspondence to: Katsutsugu Umeda, Department of Pediatrics, Graduate School of Medicine, Kyoto University, 54, Kawahara-cho, Shogoin, Sakyo-ku, Kyoto 606-8507, Japan.
E-mail: umeume@kuhp.kyoto-u.ac.jp

Received 1 May 2009; Accepted 10 August 2009

DOI 10.1002/pbc.22280
Published online 3 November 2009 in Wiley InterScience (www.interscience.wiley.com)

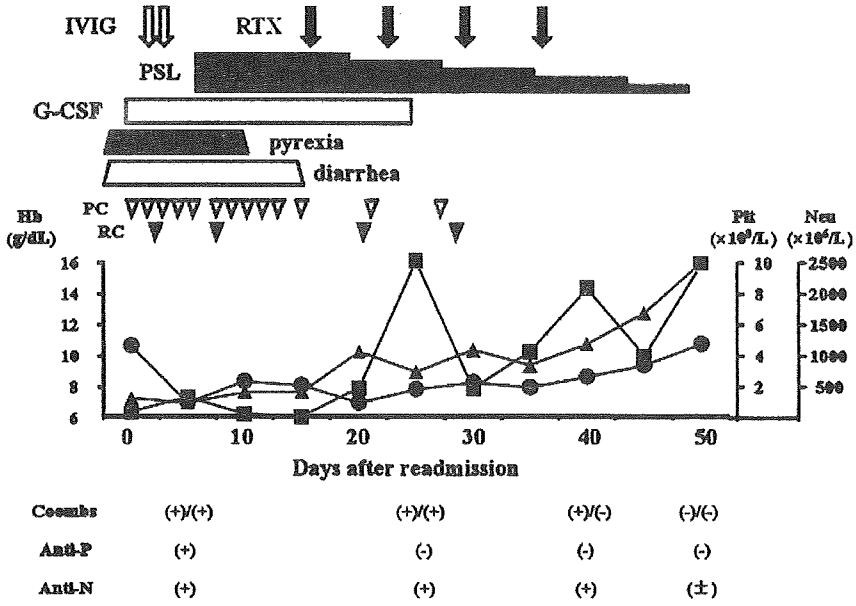

Fig. 1. The clinical course after readmission. IVIG, intravenous immunoglobulin; RTX, Rituximab; PSL, prednisolone; G-CSF, granulocyte colony-stimulating factor; RC, packed red blood cell concentrate; PC, packed platelet concentrate; Plt, platelet counts; Neu, neutrophil counts; Coombs, direct/indirect Coombs test; Anti-P, anti-platelet antibody; Anti-N, anti-neutrophil antibody. Closed circles, triangles, and squares indicate Hb levels, platelet counts (Plt), and neutrophil counts (Neu), respectively.

respectively. In an attempt to induce his return to full donor chimerism, the patient was given frozen 1.0×10^7 and 5.0×10^7 PB lymphocytes/kg on days 805 and 850, respectively, which had been harvested from the same donor who had provided the BM. Before this second DLI, the patient had not undergone any notable events such as contracting an infectious disease, medication changes or vaccinations. The clinical course after the second DLI is shown in Figure 1. Two weeks after it was delivered, the patient developed a skin rash, diarrhea, fever, elevated serum liver enzyme value, and thrombocytopenia. The patient was diagnosed clinically as having GVHD. Since restarting the patient on tacrolimus did not improve his symptoms, he was readmitted to our hospital on day 44 after the second DLI.

On readmission, the physical examination revealed no abnormal symptoms except for a persistent high fever. The results of the laboratory investigations are shown in Table I. Antibody screening tests revealed strong positivity in the direct and indirect Coombs test, and the presence of anti-platelet antibodies and anti-neutrophil antibodies specific for HNA-1a and 1b. However, other antibody screening tests were negative. There was no fungal infection or recurrence of CMV and EBV. An examination of the BM on day 896 after the BMT revealed a hypocellular marrow, but no

TABLE I. Laboratory Data on Readmission

	Value	Unit	Normal range		Value	Unit	Normal range		Value	Normal range
WBC	3.1	10^9/L	3.6–9.8	AST	38	IU/L	13–33	CMVpp65	(−)	(−)
Neu	0.93	10^9/L	1.6–6.0	ALT	36	IU/L	8–42	EBV-DNAPCR	(−)	(−)
Lymph	2.2	10^9/L	1.1–3.9	LDH	273	IU/L	129–241	Aspergillus-Ag	(−)	(−)
Hb	10.6	g/dl	11.3–13.7	ALP	473	IU/L	115–359	Candida-Ag	(−)	(−)
Reti	7.1	10^9/L	2.7–9.3	T.Bil	0.8	mg/dl	0.3–1.3	Direct Coombs Test	(+)	(−)
Plt	12	10^9/L	192–456	TP	7.3	mg/dl	6.3–8.1	Indirect Coombs Test	(+)	(−)
Haptoglobin	102.4	mg/dl	14–294	Alb	4.3	mg/dl	3.9–5.1			
CRP	4.9	mg/dl	<0.2	Soluble IL2	972	U/ml	145–519	Anti-neutrophil antibodies	(+)	(−)
β-DG	7.473	ng/ml	<11	Ferritin	7.3	ng/ml	<155	Anti-HNA-a	(+)	(−)
Endotoxin	<1.76	pg/ml	<5	Triglycerides	58	mg/dl	34–173	Anti-HNA-b	(+)	(−)
								Anti-platelet antibodies	(+)	(−)

WBC, white blood cell; Neu, neutrophil; Lymph, lymphocyte; Hb, hemoglobin; Reti, reticulocyte; Plt, platelet; CRP, C-reactive protein; β-DG, β-D-glucan; AST, aspartate aminotransferase; ALT, alanine aminotransferase; LDH, lactate dehydrogenase; ALP, alkaline phosphatase; T.Bil, total bilirubin; TP, total protein; Alb, albumin; CMVpp65, Cytomegalovirus pp65; EBV, Epstein–Barr virus; Ag, antigen; HNA, human neutrophil antigen.

evidence of malignancy or hemophagocytosis. Chimerism studies of the BM revealed 55% of the cells were composed of donor cells. Only 17% of the PB neutrophils were oxidase-positive. The patient was first treated with IVIG (1 g/kg/day for 2 days), PSL (2 mg/kg/day daily), and granulocyte colony-stimulating factor (G-CSF). Although this initial treatment resolved the pyrexia and diarrhea, the patient's pancytopenia gradually progressed and multiple transfusions became necessary. Given his refractory autoimmune pancytopenia, he was treated with RTX (375 mg/m^2/week for four consecutive weeks). The neutrophil counts rose markedly within a few days after the first RTX infusion, which was followed by the gradual increase in Hb and platelet counts. The patient became transfusion-independent after the third RTX course, and pancytopenia did not recur when the patient stopped receiving G-CSF and PSL. The hematological values normalized 21 days after the initial RTX infusion. The autoimmune antibody levels dropped during RTX treatment and eventually disappeared almost completely. Both BM chimerism studies and analysis of the oxidase-positivity of the PB neutrophils revealed 100% donor chimerism 80 days after the initial RTX infusion. Three years after the RTX treatment, the patient was alive and free of disease and showed no signs of mixed chimerism or GVHD.

DISCUSSION

Cytopenias that follow allogeneic hSCT can be immune-mediated and are frequently associated with GVHD. Autoimmune hemolytic anemia (AIHA) and immune thrombocytopenia (ITP) occur frequently, but immune-mediated cytopenias, including autoimmune neutropenia (AIN), are relatively rare [4,5]. Cytopenias are also often seen in patients after DLI and are thought to be mediated by autoimmune mechanisms, as with GVHD. In our case, pancytopenia developed soon after DLI, along with acute GVHD and the emergence of autoantibodies against multilineage blood cells. Notably, the levels of these antibodies decreased in parallel with the improvement of the pancytopenia, while the blood and BM analyses suggested that other possible causes of cytopenias, such as viral infections and hemophagocytic histiocytosis, were unlikely. However, the BM examination also showed a hypocellular marrow, which suggested that the pancytopenia did not arise from antibody-mediated cell destruction alone. Our findings suggest that autoimmunity was the major cause of the severe pancytopenia exhibited by our patient.

Most patients with autoimmune cytopenias are rescued by the administration of high-dose IVIG and standard immunosuppressive agents such as steroids [8,9]. Furthermore, RTX has been demonstrated to be useful for treating the AIHA and ITP that follow GVHD, which is refractory to conventional treatment [5,6,10–13]. However, the prognosis of patients who develop autoimmune pancytopenia remains to be determined. Page et al. [4] reported two cases that developed pancytopenia after umbilical cord blood transplantation. Despite receiving immunosuppressive treatment, including RTX, one patient continued to need the therapy while the other required a second transplantation because of pancytopenia.

Despite the fact that our patient was initially treated with PSL, high-dose IVIG, and G-CSF, and showed improvements in the other symptoms of acute GVHD, his pancytopenia progressed. Given this rapid and potentially fatal progression, we chose to start a salvage therapeutic approach rather than continue such conventional treatments, which would result in a slower response. The institution of RTX resulted in the resolution of the pancytopenia and the almost complete disappearance of the autoimmune antibodies. Furthermore, the response to RTX was already obvious 1 week after the first RTX infusion, which is consistent with a study that showed that RTX induces a prompt response in a subpopulation of patients [14].

Although no definite conclusions can be drawn from a single case with a relatively short period of follow-up, this case strengthens the hypothesis that RTX can be a beneficial treatment for refractory DLI-induced immune-mediated pancytopenia. This case suggests that further clinical research examining the merits of RTX in such cases is warranted.

REFERENCES

1. Slavin S, Morecki S, Weiss L, et al. Donor lymphocyte infusion: The use alloreactive and tumor-reactive lymphocytes for immunotherapy of malignant and nonmalignant diseases in conjunction with allogeneic stem cell transplantation. J Hematother Stem Cell Res 2002;11:265–276.
2. Kolb HJ, Schattenberg A, Goldman JM, et al. Graft-versus-leukemia effect of donor lymphocyte transfusions in marrow grafted patients. Blood 1995;86:2041–2050.
3. Collins RHJR, Shpiberg O, Drobyski WR, et al. Donor leukocyte infusions in 140 patients with relapsed malignancy after allogeneic bone marrow transplantation. J Clin Oncol 1997;15:433–444.
4. Page KM, Mendizabal AM, Prasad VK, et al. Posttransplant autoimmune hemolytic anemia and other autoimmune cytopenias are increased in very young infants undergoing unrelated donor umbilical cord blood transplantation. Biol Blood Marrow Transplant 2008;14:1108–1117.
5. Raj K, Narayanan S, Auguston B, et al. Rituximab is effective in the management of refractory autoimmune cytopenias occurring after allogeneic stem cell transplantation. Bone Marrow Transplant 2005;35:299–301.
6. Zaja F, Bacigalupo A, Patriaca F, et al. Treatment of refractory chronic GVHD with rituximab: A GITMO study. Bone Marrow Transplant 2007;40:273–277.
7. Kojima S, Matsuyama T, Kato S, et al. Outcome of 154 patients with severe aplastic anemia who received transplants from unrelated donors: The Japan Marrow Donor Program. Blood 2002;100:799–803.
8. Cines DB, Bussel JB. How I treat idiopathic thrombocytopenic purpura (ITP). Blood 2005;106:2244–2251.
9. Gehrs BC, Friedberg RC. Autoimmune hemolytic anemia. Am J Hematol 2002;69:258–271.
10. Stasi R, Pagano A, Stipa E, et al. Rituximab chimeric CD20 antibody treatment for adults with chronic idiopathic thrombocytopenic purpura. Blood 2001;98:952–957.
11. Ratanatharathorn V, Carson E, Reynolds C, et al. Anti-CD20 chimeric monoclonal antibody treatment of refractory immune-mediated thrombocytopenia in a patient with chronic graft-versus-host disease. Ann Intern Med 2000;133:275–279.
12. Hongeng S, Tardong P, Worapongpaiboon S, et al. Successful treatment of refractory autoimmune hemolytic anaemia in a post-unrelated bone marrow transplant paediatric patient with Rituximab. Bone Marrow Transplant 2002;29:871–872.
13. Corti P, Bonanimi S, Vallinoto C, et al. Rituximab for immune hemolytic anaemia following T and B cell depleted hematopoietic stem cell transplantation. Acta Haematol 2003;109:43–45.
14. Mohty M, Marchetti N, El-Cheikh J, et al. Rituximab as salvage therapy for refractory chronic GVHD. Bone Marrow Transplant 2008;41:909–911.

Pediatr Blood Cancer 2009;53:1324–1326

BRIEF REPORT

Cytomegalovirus Infection Mimicking Juvenile Myelomonocytic Leukemia Showing Hypersensitivity to Granulocyte–Macrophage Colony Stimulating Factor

Hiroshi Moritake, MD, PhD,[1]* Toshio Ikeda, MD,[1] Atsushi Manabe, MD,[2] Sachiyo Kamimura, MD,[1] and Hiroyuki Nunoi, MD, PhD[1]

We describe an infant with cytomegalovirus (CMV) infection presenting as transient myeloproliferation resembling juvenile myelomonocytic leukemia (JMML). The patient fulfilled the international diagnostic criteria of JMML, including hypersensitivity to granulocyte–macrophage colony-stimulating factor (GM-CSF). Viral studies using serologic assays and polymerase chain reaction (PCR) were positive for CMV. Clinical symptoms disappeared and laboratory values returned to normal without specific treatment within 1 year. Follow-up showing a decrease in viral titers suggested CMV infection as an etiologic factor for the development of myeloproliferative features. We conclude that the CMV infection transiently induced abnormal myelopoiesis in this infant. Pediatr Blood Cancer 2009;53:1324–1326. © 2009 Wiley-Liss, Inc.

Key words: cytomegalovirus; juvenile myelomonocytic leukemia; GM-CSF hypersensitivity

INTRODUCTION

The majority of prenatal and postnatal cytomegalovirus (CMV) infections are asymptomatic in newborn periods; however, clinical features of symptomatic CMV infection often overlap other hematologic diseases. Juvenile myelomonocytic leukemia (JMML) is a myeloproliferative/myelodysplastic disorder that primarily affects children younger than 5 years of age. However, there are several reports describing difficulties in discriminating between JMML and infectious diseases [1,2]. The diagnosis of JMML is based on the presence of defined diagnostic criteria including a characteristic hypersensitivity of myeloid progenitors to granulocyte–macrophage colony-stimulating factor (GM-CSF) [2]. We present a case with CMV infection showing GM-CSF hypersensitivity mimicking JMML.

CASE REPORT

A 2-month-old Japanese female with a 1 month history of failure to thrive and repeated infections was referred to our hospital. Physical examinations revealed hepatosplenomegaly with the liver descended 5 cm below the right costal margin and the spleen 4 cm below the left costal margin. Laboratory data showed a white blood cell count of 12.9×10^9/L; hemoglobin, 10.4 g/dl; and platelets, 265×10^9/L. The differential count showed elevated monocytes and immature granulocytes (23% neutrophils, 49% lymphocytes, 4% eosinophils, 14% monocytes, 7% myelocytes, and 3% metamyelocytes). Hemoglobin F was normal at 30.8% (normal range for age: 25–60%). Serologic tests and/or polymerase chain reaction (PCR) analysis for Epstein–Barr virus (EBV), human herpesvirus (HHV)-6, and parvovirus B19 were negative. IgM titer for CMV by enzyme linked immunosorbent assay was positive and the existence of CMV infection was further confirmed by PCR.

The bone marrow was hypercellular with a myeloid/erythroid ratio of 4.6:1. Blasts and promyelocytes comprised 0.4% of nucleated cells. No myelodysplasia was seen in the bone marrow. Karyotyping of marrow cells revealed 46XX, with no Philadelphia chromosome or monosomy 7. To differentiate JMML from CMV infection, in vitro culture assays of bone marrow and peripheral blood were examined [3]. The results showed spontaneous proliferation of predominantly monocytic/macrophage colonies. In vitro assays showed the patient's cells were hypersensitive to GM-CSF (Table I).

Though the patient fulfilled the criteria of JMML [2], no specific treatment was required because no sign of progressive disease was seen. The patient was closely monitored and her clinical course was unremarkable with gradual resolution of hepatosplenomegaly and blood counts. Peripheral blood monocyte count dropped below

TABLE I. Spontaneous CFU-GM Formation and GM-CSF Dose–Response Analysis From Patient Samples

GM-CSF (ng/ml)	Peripheral blood (normal range)	Bone marrow (normal range)
0	73 (0–8)	78 (0–3)
0.01		103 (1–6)
0.1		118 (3–6)
1		129 (5–14)
10		126 (23–46)

The colony assays were performed as previously described [3]. The depletion of monocytes was employed for bone marrow cells. 1×10^5 cells were used for peripheral blood whereas 2×10^4 cells were cultured for bone marrow cells. CFU-GM, colony forming unit-granulocyte and macrophage; GM-CSF, granulocyte–macrophage colony-stimulating factor.

Additional Supporting Information may be found in the online version of this article.

[1]Division of Pediatrics, Faculty of Medicine, Department of Reproductive and Developmental Medicine, University of Miyazaki, Miyazaki, Japan; [2]Department of Pediatrics, St. Luke's International Hospital, Tokyo, Japan

*Correspondence to: Hiroshi Moritake, Division of Pediatrics, Faculty of Medicine, Department of Reproductive and Developmental Medicine, University of Miyazaki, Miyazaki 889-1692, Japan.
E-mail: moritake@fc.miyazaki-u.ac.jp

Received 23 March 2009; Accepted 27 July 2009

DOI 10.1002/pbc.22253
Published online 3 September 2009 in Wiley InterScience (www.interscience.wiley.com)

TABLE II. Serial Evaluation of Peripheral Blood Counts and Viral Titers for Cytomegalovirus

	1/22/2002	1/29/2002	2/7/2002	2/14/2002	2/26/2002	4/16/2002	7/4/2002
Hemoglobin (g/dl)	10.4	9.8	9.9	10.1	10.1	12.8	14.2
WBC count ($\times 10^3/\mu l$)	12.9	15.6	14.6	15.6	8.9	10.8	8.9
Platelet count ($\times 10^3/\mu l$)	265	384	352	345	244	443	325
Differential leukocyte count (%)							
Neutrophils	23	20	22	32	16	15	15
Lymphocytes	49	62	50	46	69	71	74
Eosinophils	4	0	4	0	5	6	2
Monocytes	14	11	18	12	8	8	8
Basophils	0	0	0	2	1	0	1
Myelocytes	7	3	2	2	0	0	0
Metamyelocyte	3	3	4	6	1	0	0
Blasts	0	0	0	0	0	0	0
Cytomegalovirus IgM	3.94		3.39		2.92	1.01	0.55

1×10^9/L at 3 months of age, and hepatosplenomegaly disappeared at 9 months. A fall in viral titers for CMV was also observed during follow-up (Table II). After a follow-up of 2 years, the patient is well at 26 months of age with no sign of hepatosplenomegaly, and has completely normal blood counts.

DISCUSSION

CMV infection is commonly associated with hematologic abnormalities including leukocytosis with atypical lymphocytes, hemolytic anemia, and thrombocytopenia. JMML is known to be mimicked by a variety of infectious organisms, including EBV [4], HHV-6 [5], parvovirus B19 [6], and CMV. However, there are three reports of progressive cases where infants suffered from JMML in spite of a diagnosis of CMV infection [1,7,8]. Although it is important to differentiate JMML from an infectious disease, definite discrimination is often very difficult. Since half the children with JMML have evidence of some clonal disorder, in cases with no clonal abnormality, caution should be taken in making a diagnosis of JMML. Tartaglia et al. [9] reported that a somatic mutation in PTPN11 is responsible for oncogenesis in JMML. Further exploration of mutations in genes involved in the RAS/MAPK pathway (NRAS, KRAS2, NF1, and PTPN11) may be helpful to confirm a diagnosis of JMML. Our case spontaneously recovered a normal blood count and has survived more than 2 years without any treatment for JMML after the hematologic abnormalities were detected, even though hypersensitivity to GM-CSF, which is believed to be critical for the diagnosis of JMML, was seen. Our patient had three characteristics that were inconsistent with JMML. First, elevation of hemoglobin F above the normal range was not detected. Second, thrombocytopenia was not seen throughout the clinical course. Finally, dysplastic features were not found. These findings may be helpful in distinguishing infection from JMML. Recently, Koetecha et al. [10] published that GM-CSF induced phosphorylated STAT5 could be detected by flow cytometry-based signaling assays in JMML cells, but not from other childhood myeloprolifearative disorders. Furthermore, Gaipa et al. [11] described three JMML case reports using similar method and confirmed that its application in JMML might represent a new integrated diagnostic tool. They suggest the JAK-STAT signaling pathway has a critical role in the biologic mechanism of JMML. We also investigated GM-CSF-induced phosphorylation of STAT5 in our patient's frozen bone marrow sample and compared it with the monocytic cell line U937 that expresses a PTPN11 exon 3 mutation, as well as a frozen bone marrow sample from a normal healthy volunteer. We used phosphospecific flow cytometry after exposure to increasing concentrations of GM-CSF according to their methods. The expression of a phosphorylated STAT5 population in samples from our patient or a healthy volunteer was minimal compared to the reaction seen in U937 cells (Supplemental Fig. 1), consistent with their reports. Elucidation of these molecular mechanisms will contribute to a definitive differentiation between JMML and mimicking cases.

ACKNOWLEDGMENT

We are grateful to Dr. Kaede Yanagita for her useful comments on this manuscript.

REFERENCES

1. Kirby MA, Weitzman S, Freedman MH. Juvenile chronic myelogenous leukemia: Differentiation from infantile cytomegalovirus infection. Am J Pediatr Hematol Oncol 1990;12:292–296.
2. Niemeyer CM, Fenu S, Hasle H, et al. Differentiating juvenile myelomonocytic leukemia from infectious disease [letter]. Blood 1998;91:365–367.
3. Emanuel PD, Bates LJ, Castleberry RP, et al. Selective hypersensitivity to granulocyte–macrophage colony-stimulating factor by juvenile chronic myeloid leukemia hematopoietic progenitors. Blood 1991;77:925–929.
4. Herrod HG, Dow LW, Sullivan JL. Persistent epstein–barr virus infection mimicking juvenile chronic myelogeneous leukemia: Immunologic and hematologic studies. Blood 1983;61:1098–1104.
5. Lorenzana A, Lyons H, Sawaf H, et al. Human herpesvirus 6 infection mimicking juvenile myelomonocytic leukemia in an infant. J Pediatr Hematol Oncol 2002;24:136–141.
6. Yetgin S, Cetin M, Yenicesu I, et al. Acute parvovirus B19 infection mimicking juvenile myelomonocytic leukemia. Eur J Haematol 2000;65:276–278.
7. Wilson DB, Michalski JM, Grossman WJ, et al. Isolated CNS relapse following stem cell transplantation for juvenile myelomonocytic leukemia. J Pediatr Hematol Oncol 2003;25:910–913.

8. Toyoda H, Ido M, Hori H, et al. A case of juvenile myelomonocytic leukemia with concomitant cytomegalovirus infection. J Pediatr Hematol Oncol 2004;26:606–608.
9. Tartaglia M, Niemeyer CM, Fragale A, et al. Somatic mutations in PTPN11 in juvenile myelomonocytic leukemia, myelodysplastic syndromes and acute myeloid leukemia. Nat Genet 2003;34:148–150.
10. Kotecha N, Flores NJ, Irish JM, et al. Single-cell profiling identifies aberrant STAT5 activation in myeloid malignancies with specific clinical and biologic correlates. Cancer Cell 2008;14:335–343.
11. Gaipa G, Bugarin C, Longoni D, et al. Aberrant GM-CSF signal transduction pathway in juvenile myelomonocytic leukemia assayed by flow cytometric intracellular STAT5 phosphorylation measurement. Leukemia 2009;23:791–793.

Gene 432 (2009) 7–18

Contents lists available at ScienceDirect

Gene

journal homepage: www.elsevier.com/locate/gene

Genomic organization of regions that regulate chicken glycine decarboxylase gene transcription: Physiological and pathological implications

Hiroshi Kawaguchi, Soshi Okamoto [1], Dwaipayan Sikdar, Akihiro Kume [2], Fang Li [3], Omar Mahmoud Mohamed Mohafez, Mohammed Hassan Shehata, Koichi Hiraga *

The Department of Biochemistry, University of Toyama Graduate School of Medicine and Pharmaceutical Sciences, 2630 Sugitani, Toyama 930-0194, Japan

ARTICLE INFO

Article history:
Received 31 July 2008
Received in revised form 5 November 2008
Accepted 7 November 2008
Available online 24 November 2008

Received by A. Bernardi

Keywords:
Promoter
Upstream regulator regions
Cell-type specificity
Glycine catabolism
Active one-carbon
Nonketotic hyperglycinemia

ABSTRACT

Regions required for chicken glycine decarboxylase gene transcription were examined. A region between −82 and +22 (−82/+22) with motifs similar to binding sites for Sp1, NF-Y and CP2 was assigned to the proximal promoter active in both chicken hepatoma cell line, LMH, and hepatocytes in primary culture. In LMH cells, a genomic region, KX, between KpnI (−4155) and XbaI (−2113) sites changed promoter activity with the aid of four additional genomic regions termed *up*stream *r*egulator regions for *s*uppression (UpRS) and *a*ctivation (UpRA) of transcription. Those precise segments are UpR1S (−376/−346), UpR1A (−345/−291), UpR2S (−137/−108) and UpR2A (−107/−83). Within KX, −4155/−3605 activates and −3604/−3367 suppresses the promoter. −3366/−3024 activates or suppresses the promoter, probably with different UpR counterparts. −2197/−2113 restores the actions of −3366/−3024. While in LMH cells, the upstream UpRs abrogate the functions of immediately downstream UpRs, UpR1S or UpR2S or both may be at least less active in hepatocytes than in LMH cells. Nuclear extracts from various chicken tissues and LMH cells had UpR2A binding proteins in different populations, suggesting that together with the UpRs, the segments in KX are involved in the regulation of cell type-specific transcription of this gene.

1. Introduction

Glycine decarboxylase (GDC) [EC 1.4.4.2] (Hiraga and Kikuchi, 1980a,b), which was initially termed P-protein as reviewed by Kikuchi and colleagues (Kikuchi, 1973; Kikuchi and Hiraga, 1982; Kikuchi et al., 2008) constitutes the glycine cleavage system together with two other intrinsic components, the carrier protein of an aminomethyl group and hydrogen (H-protein) and tetrahydrofolate-requiring protein (T-protein), and a common lipoamide dehydrogenase. GDC, which catalyzes the initial decarboxylation of oxidative glycine degradation, requires two types of functions of H-protein. First, GDC, a potential enzyme by itself, is converted to an active decarboxylase by H-protein. Second, the decarboxylation product, aminomethyl carbanion, is captured by the prosthetic lipoyl moiety of H-protein in association with the reductive cleavage of its disulfide bond for further breakdown to NH_3 and N^5, N^{10}-methylene-tetrahydrofolate by T-protein (Hiraga and Kikuchi, 1980b; Kikuchi and Hiraga, 1982; Kikuchi et al., 2008). The reaction catalyzed by T-protein finally yields the reduced form of the prosthetic lipoic acid, which is recycled through oxidation by lipoamide dehydrogenase in the presence of NAD^+. This overall reaction is the major pathway for glycine degradation in vertebrates (Kikuchi, 1973) and supplies tetrahydrofolate derivatives indispensable for the biosynthesis of purine nucleotides, thymidylate, methionine, lipids and other cellular substances.

Livers of uricotelic animals exhibit the highest specific activity of glycine cleavage reaction in the vertebrate tissues examined (Kikuchi, 1973; Kikuchi et al., 2008; Kure et al., 1991a,b), probably because purines are involved in the pathway for NH_3 excretion. In chicken tissues, the specific activity of glycine cleavage reaction was determined in the liver, kidney, and brain in a ratio of 100:30:3. GDC mRNA levels in these tissues were proportional to this ratio. Heart and spleen tissues are inactive in glycine cleavage reaction due to negligible levels of GDC. Run-on transcription analysis revealed that the tissue-specific GDC levels are predominantly determined at the level of transcription (Kure et al., 1991a,b). In 16-day chick embryo livers, the levels of specific activity, polypeptide and mRNA of GDC were approximately 10% of those in adult chicken livers and began to increase at late embryonic stages. Eventually, GDC increased to the adult level after hatching due to increased transcription of the GDC gene (Matsui et al., 1993). In other words, GDC gene transcription may

Abbreviations: GDC, glycine decarboxylase; UpRA and UpRS, *up*stream regulator regions for *a*ctivation and *s*uppression of transcription.

* Corresponding author. Tel.: +81 76 434 7225; fax: +81 76 434 5014.
E-mail address: hiragak@med.u-toyama.ac.jp (K. Hiraga).
URL: http://www.med.u-toyama.ac.jp/bmb/index.html (K. Hiraga).
[1] Present address: The Department of Neurosurgery, University of Toyama School of Medicine, Japan.
[2] Present address: The Division of Genetic Therapeutics, Jichi Medical School, Tochigi 329-0498, Japan.
[3] Present address: Institute of Molecular Biosciences, Massey University, Palmerston North, New, Zealand.

0378-1119/$ – see front matter © 2008 Elsevier B.V. All rights reserved.
doi:10.1016/j.gene.2008.11.014

be increasingly changed in the embryonic and neonatal livers and constitutively maintained at the maximally increased level in the adult liver. Moreover, GDC gene transcription is less active in the kidney and brain than in the liver, and inactive in the heart and spleen. These properties imply that the availability of *trans*-factors required for GDC gene transcription regulation presumably changes in response to the statuses of tissue differentiation to provide conditions appropriate for glycine catabolism.

Concerning GDC gene structure, we characterized part of a 5′-exon in a chicken genomic DNA clone, pCPG301EE2.8 subcloned from λCPG301, to determine the translation start site, since the initially cloned chicken GDC cDNA was a truncated form with no translation start codon (Kume et al., 1991). The isolation of chicken GDC cDNA clones helped to clone a human version of GDC cDNA (Kume et al., 1991). Sakakibara et al. (1990) further clarified that the human genome possesses true and processed GDC genes, which were respectively assigned to 9p23–24 and 4q12 (Isobe et al., 1994). In humans, a defective glycine cleavage system causes nonketotic hyperglycinemia (Kikuchi, 1973; Kikuchi and Hiraga, 1982; Nyhan, 1989; Kikuchi et al., 2008). Most patients with this disease had a molecular lesion in GDC and therefore in its genes (Kume et al., 1988; Sakakibara et al., 1990; Kure et al., 1991a,b; Takayanagi et al., 2000; Kure et al., 2006; Kanno et al., 2007). Notably, Sakakibara et al. (1990) identified for the first time that the GDC gene of a patient with this disease had been deleted at a 5′-region. A recent study has confirmed that the deletion including a 5′-region of the human GDC gene is a major cause of nonketotic hyperglycinemia (Kanno et al., 2007). In this context, GDC genes have been identified from various micro-organisms (Wilson et al., 1993; Okamura-Ikeda et al., 1993; Nakai et al., 2005) and their structures can be seen in several databases. In *Escherichia coli*, a LysR family protein regulates the biosynthesis of the components of the glycine cleavage system (Wilson and Stauffer, 1994). In *Saccharomyces cerevisiae*, a genomic region with a core element, CTTCTT, was required for induction of the yeast homolog of GDC under nutritionally restricted conditions (Hong et al., 1999; Sinclair et al., 1996). However, regulation mechanisms directing vertebrate GDC gene transcription were largely unknown. Taking the features of chicken GDC gene transcription into account, we attempted to structurally and functionally characterize genomic regions that may be involved in chicken GDC gene transcription regulation.

2. Materials and methods

2.1. DNA clones, plasmids, cells and RNA

Chicken genomic DNA subclones constructed with pBluescript from λCPG301 (Fig. 1A) (Kume et al., 1991; Yamamoto et al., 1991) were used. A chicken hepatoma cell line, LMH (JCRB0237) (Kawaguchi et al., 1987), was obtained from the Health Science Research Resources Bank (Osaka, Japan) and maintained in Waymouth MB752/1 medium containing 10% fetal bovine serum at 37 °C and under 5% CO_2 in air. Chickens at 4 months of age were also used. Total RNA was prepared from chicken livers and LMH cells as described (Chomczynski and Sacchi, 1987). pGL3-basic and pRL-SV40 vectors (Promega Corp.) and other reagents were from local distributors.

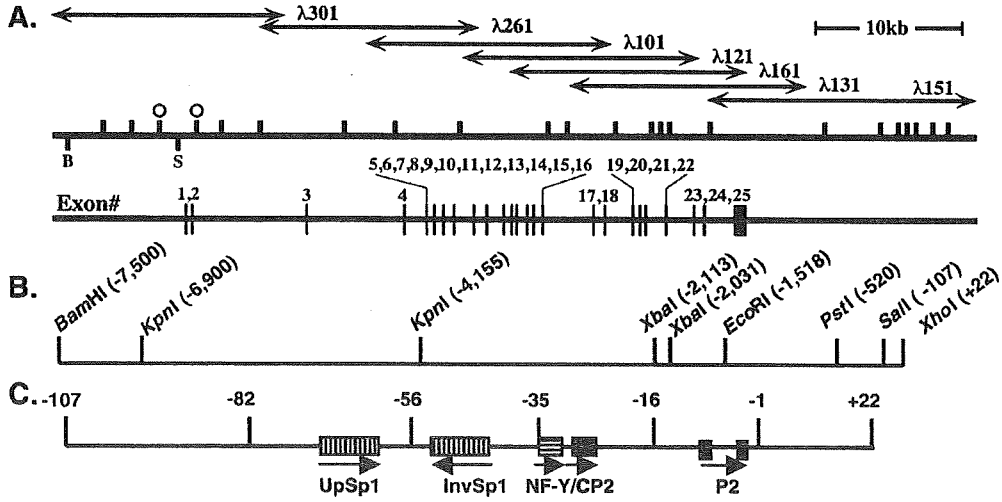

D.

```
-540 ctctgcccaa gccacctgca gatgttcact gtagggcact gtaaagattt tggtacaaag
-480 tgctgggcag tgttaaggga ttgaacactt cagatgaaga cacagcaatg catgtgtacg
-420 tacacagcag catcacagtg ccatcttaaa ctgctgggtc ctctgggaaa atttattagc
-360 gctgcaaaac taagagaaga tggaggctgt ggtggccctt tgcagcccag cagaattgca
-300 cactagatgg ccatcggtgg tgcggccagg cgcggtgcag ccttgccccc tcctcagaga
-240 tgcgcacaaa gcgccgggtg ggatgaatct ttccttatct gctccgacag ccccaggccg
-180 gagggcaacg caaagcccgg ccatctccgc atccccgcgc ggccggagcg gggtcagggc
-120 cgagcgggtc gggtcgactc ggccgggggc gtggggatca ggtggcggcg aggcgggggcg
 -60 agcgcggcac cgcctcctcct ccccattggc gctggcggcg ggggccgcgc cgcaccgccc
  +1 TCCCCGGCCA CAAAGCGTGG TGCCGGACGG CGGCGGTGGG GCGGTGTTAG CGGGGTCATG
```

Fig. 1. Genomic organization of the chicken GDC gene. (A) The outline of the cloned GDC gene. Genomic DNA fragments of λclones (arrows), recognition sites for EcoRI on the DNA stretch (vertical graduations on the bold line), those for BamHI (B) at −7.5 kb and SalI (S) at −107, pCPGEE2.8 insert (the region between open circles), and locations of 25 exons in red are shown. (B) Recognition sites by several restriction enzymes are shown along with the 5′-flanking sequence. (C) *Cis*-elements in the proximal promoter. Positions (nucleotide numbering) and directions (arrows) are shown. UpSp1 and InvSp1 denote the inverted repeats of Sp1 sites. (D) The nucleotide sequence from −540 to +60. UpR1S (−376/−346) and UpR2S (−137/−108), and UpR1A (−345/−291) and UpR2A (−107/−83) are shown in blue and red, respectively. UpSp1 and InvSp1 are underlined. Lowercase and uppercase letters indicate the 5′-flanking region and part of exon 1. Translation start codon is from +58 to +60. Accession number of the nucleotide sequence from −4160 to −1 is AB245436.

2.2. Recombinant plasmids carrying promoter regions

The region between the BamHI and SalI sites within the λCPG301 insert (the region between B and S in Fig. 1A) was subcloned as pBS. Note that the pBS insert is referred to as the genomic region −7500/−108 in Table 2. The 5′ primer, 5′-GGG CCG AGC GGG TCG GGT CGA CTC GG-3′ (−124 to −99) encompassing the underlined internal SalI site at −107, and the 3′ primer complementary to a sequence from +1 to +22 of chicken GDC cDNA (5′-GGC TCG AGC ACC ACG CTT TGT GGC CGG GGA-3′) with the underlined artificial XhoI site were used to amplify the −107/+22 region on a pCPGEE2.8 template by PCR. A product subcloned at the EcoRV site in pBluescript in an appropriate orientation was cut at XhoI sites in the 3′ primer and multiple cloning sites to remove a SalI site between them. The insert of the self-ligation product (pSX) was termed −107/+22. The pBS insert was transferred to pSX using BamHI and SalI sites, yielding a subclone carrying the 7.5-kb-long genomic region upstream from +22. The required flanking regions between appropriate sites for restriction enzymes (see Fig. 1B) and the XhoI site were subcloned with a pGL3-basic vector. −107/+22 in the pGL3 vector was unidirectionally deleted by the method of Henikoff (1984) to prepare subclones each carrying −82/+22, −56/+22, and −35/+22. Nucleotide sequences were determined using various synthetic DNA primers and an automated DNA sequencer, Prism 310 (Applied Biosystems Japan).

2.3. Transcription start site

Primer 1 (5′-GCG CCC GCA GCT CTG CAT GA-3′) (Tm=58 °C in 75 mM KCl) was synthesized as a strand complementary to chicken GDC mRNA. Its 5′-end base is complementary to that 18 bases downstream from the adenine base of the translation start codon in the reported chicken GDC cDNA sequence (Kume et al., 1991) and to that at +75 in the complete exon 1 sequence determined in the present study. The CAT near the 3′-end of primer 1 is complementary to the translation start codon shown in Fig. 1D. The 5′-end of 20-mer primer 2 was 123 bp downstream from that of primer 1. Primer extension (Calzone et al., 1987) was performed with 5′-end-labeled primer 1 or 2 ([^{32}P]-primer 1 or 2), chicken liver total or poly(A)$^+$ RNA (20 to 2 μg) and a reverse transcriptase. For S1 protection assay, a 182-base-long single-strand DNA probe was replicated from [^{32}P]-primer 1 on a pCPG301EE2.8 template cleaved in advance at the −107 SalI site. The probe DNA was separated from the template plasmid by electrophoresis on a gel containing 7 M urea. The probe DNA was annealed at 60 °C for 2 h with liver poly(A)$^+$ RNA (2 μg) denatured in advance at 90 °C for 2 min, and then digested with S1 nuclease (5 U/ml) for 5 to 90 min at 37 °C. Products from primer extension and S1 protection reactions were simultaneously resolved on the denatured gel together with aliquots of mixtures for sequencing reactions that also began with [^{32}P]-primer 1 on the pCPG301EE2.8 insert. Products were located on XAR5 films (Kodak) or a BAS2000 imaging analyzer (Fuji Film Co. Ltd., Tokyo).

2.4. Electrophoretic mobility shift assay

Nuclear fractions isolated from LMH cells and chicken livers (Hibino et al., 2006) were extracted with a buffer containing 0.3 M NaCl by the method of Dignam et al. (1983) and stored at −80 °C until use in electrophoretic mobility shift assay (EMSA). Aliquots of the nuclear extract (1 to 5 μg in protein amounts) were incubated with radioactive genomic or synthetic DNA probes (20,000 cpm) for 20 min at room temperature in a reaction mixture containing, in a final volume of 15 μl, 10 mM Tris–HCl buffer, pH 7.5, 40 mM NaCl, 1 mM EDTA, 1 mM dithiothreitol, 6 mM $ZnCl_2$, 0.4 μg of poly [dI-dC], 0.5 mM PMSF, and 4% glycerol (Hennighausen and Lubon, 1987). For competition assay, the nuclear extract was treated with 200 molar excess competitors at room temperature for 20 min prior to addition of [^{32}P]-DNA probes. DNA/protein complexes were resolved on a 4% polyacrylamide gel containing 6.7 mM Tris–HCl buffer, pH 7.5, 3.3 mM sodium acetate, and 1 mM EDTA and located on autoradiograms.

2.5. Site-directed mutagenesis

Base substitutions were introduced using a Mutan-Super Express Km kit (Takara Bio, Japan) according to manufacturer's instructions. The mutants with a confirmed nucleotide sequence were used for promoter assays. Double-stranded UpR2A sequences with three-nucleotide substitutions were chemically synthesized for use in EMSA or ligated with −82/+22 in a pGL3-basic vector to prepare mutant −107/+22 constructs.

2.6. Chick hepatocyte primary culture

This was performed by the method of Seglen (1976). Chicks at 5 weeks of age were anesthetized and killed by cervical incision. The liver was perfused with 250 ml of Mg^{2+}- and Ca^{2+}-free Hanks' solution, followed by perfusion with 400 ml of HEPES-NaOH buffered saline (pH7.5) containing 50 mg/ml of collagenase at 37 °C. Dispersed cells were suspended with Hanks' solution. Hepatocytes collected by centrifugation at 60 ×g for 2 min were dispersed with Waymouth MB752/1 medium containing 10% fetal bovine serum, and maintained with the medium supplemented with 10 μM dexamethasone and 100 nM insulin under 5% CO_2 in air at 37 °C for 9 days by changing the culture medium at 24-h intervals to assay for promoter activity in hepatocytes.

2.7. Transient expression of luciferase gene

Wild-type and recombinant pGL3-basic and pRL-SV40 vectors were isolated by CsCl equilibrium centrifugation and transfected to LMH cells and hepatocytes by lipofection using Tfx-50 (Promega Corp.). Four cultures of LMH cells and hepatocytes received identical constructs under comparable conditions and were respectively lysed following 40 h- and 72 h-incubations. The lysates were assayed for firefly and *Renilla* luciferase on a Dual-luciferase Reporter Assay System (Promega Corp.) and a luminometer, Luminous CT-9000 (DiaYatron, Tokyo). Promoter activities were expressed as a mean value of four assays±SD.

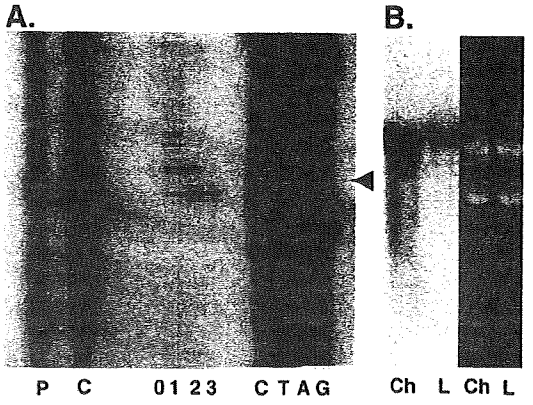

Fig. 2. Transcription start site. (A) The product extended from [^{32}P]-primer 1 (lane P) and the single-strand DNA probe prepared from [^{32}P]-primer 1 and protected from S1 nuclease digestion for 0, 30, 60, and 90 min (lanes 0, 1, 2, and 3) were resolved by electrophoresis on a denatured gel. Sequencing ladders also begin with [^{32}P]-primer 1 (lanes C, T, A, G). An arrowhead indicates thymine base at the transcription start site. (B) Northern blot analysis. Chicken liver (lane Ch) and LMH cell (lane L) total RNA (10 μg) were probed with [^{32}P]-GDC cDNA (left). RNA staining with ethidium bromide is shown (right).

Table 1
Boundary sequences of 25 exons

Exon/intron boundary sequence			
Exon	(bp)	5′ End	3′ End
1	282	cgcaccgcccTCCCCGGCCA	CGGGGTGCAGgtgggtgcct
2	79	ttctttgcagAGCGTCGAGG	GACCACGTCGgtaaattgcc
3	136	tctcaattagTTGAAAATGA	ACGCAGGATGgtaatgtaca
4	165	ttccttacagGGTTACCCAG	TATGTCACAGgtactatgtt
5	76	tttttaacagGCAAAACAAA	CTAGAGCAAAgtatgttctt
6	148	tgttttccagTTATACAGGT	TCAGAATGGGgtaaagtaaa
7	197	cctcctcagACTCTTGCCT	GCGTTACAAGgtaaaggctc
8	97	tgtgtcttagAGATGCAAAT	CACTGCACAGgtgactcatc
9	106	ggatccttagGCTCTCCTGG	CTGGCGGAGGgtcgaatatt
10	140	tgttttatagGTCTCAGACG	TGATGGCAGAgtaagcaacc
11	81	ttgcccatagCTTGGAGTAT	GTCTTCAGCTgtaagtggac
12	98	tgtgtcaaagGAACTAGTTG	TTTTCAACAGgttttgtgaa
13	85	tgtcctccagCTATCACTCC	GATTCCTTTGgtgggtattt
14	42	ctatttttagGGGTCCTGTA	TGAACTTGCGgtaagttgaa
15	143	tttgtttaagCCGATTTCAT	AACCAAACAGgtaggaattt
16	76	cctcttgcagTGGAGCCCAA	TCATAGAAGTgtaagtgtca
17	126	tccttccaagGTTTGCCTTA	AAAAGCAATGgtgagtattt
18	150	ctgcctccagGTGGACAAGC	GAATGCACAGgtatgcagtc
19	113	cactttacagGTGGGTCTGT	CAATTGGAGTgtaagtatat
20	142	tttgttttagGAAGAAACAT	GTATATCAAGgtgtgtagac
21	112	ctcttttcagACAATGGGAG	GGAGTAAGAGgcaagtagtg
22	96	ttccttacagGTTACGTAGC	CAGGATTATGgttagtcaaa
23	173	ctgttttcagGTTTTCATGC	CCCTCTGAAGgtaagatggc
24	81	ctgcttgcagATGTCACCAC	ATTCCCACTGgtgagtaaac
25	628	ctgcatttagCCTTTTGTGA	GGTCAGAATTaagtatcatg

Exon/intron boundary sequences are shown for all exons (uppercase letters), and 5′-flanking sequence and introns (lowercase letters) together with the lengths of exons in bp. Chicken GDC cDNA sequence can be seen with accession numbers D90266, M64402 or NM_204322.

2.8. Chicken GDC gene locus

AB245436 is a 4220 bp chicken genomic sequence between the KpnI site at −4155 (Fig. 1C) and the 3rd base of the translation initiation codon in exon 1 (Fig. 1D). Various segments of AB245436 and a chicken cDNA sequence (NM_204322) were aligned over chicken genomic regions using tools, Blat and Blast, accessible from the UCSC Genome Bioinformatics Site (http://genome.ucsc.edu/) and National Center for Biotechnology Information (http://blast.ncbi.nlm.nih.gov/Blast.cgi). Deposits related to ENSGALG00000015053 that identifies the chicken gene for GCSP were examined for the correctness, since GCSP is an alternative name of GDC of the glycine cleavage system. Human and chicken genome databases were also searched using the two tools for sequences similar to the chicken UpRs. Putative *cis*-elements were searched using a tool, Patch, at gene-regulation. com (http://www.gene-regulation.com/).

3. Results

3.1. Transcription start site

In the previous study, we determined that the translation start codon was downstream from the unique SalI site in a 2.8-kb chicken GDC gene fragment subcloned from λCPG301 as pCPG301EE2.8 (the region between open circles in Fig. 1A) (Kume et al., 1991). In the present study, we tried to determine the transcription start site and exon/intron boundaries of this gene. In primer extension analysis using chicken liver total RNA, a major 75-base-long product (lane P in Fig. 2A) was reverse-transcribed from [^{32}P]-primer 1. Under comparable conditions but using chicken liver poly(A)$^+$ RNA, an approximately 200-base-long product extended from [^{32}P]-primer 2 (not shown). The two products were thought to extend to similar endpoints on GDC mRNA, since primer 2 begins with the base 123 bases downstream from the 5′-end of primer 1. For S1 nuclease mapping, a 182-base-long single-stranded genomic DNA was replicated from [^{32}P]-primer 1 to the SalI site on pCPG301EE2.8 (see Experimental Procedures) and annealed with liver poly(A)$^+$ RNA. The 75 bases long product was again protected from digestion of the hybrid with S1 nuclease. Its signal intensity clearly increased accordingly to the prolonged digestion (Fig. 2A, lanes 0, 1, 2, and 3). The products from primer extension and S1 protection assays electrophoretically migrated to a position corresponding to the thymine base indicated with an arrowhead beside the sequencing ladders, which also begin from [^{32}P]-primer 1. These findings imply that chicken GDC gene transcription may mainly begin with this thymine base that is 57 bases upstream from the adenine nucleotide of the translation start codon in exon 1 (Fig. 1D), although at present we cannot rule out the possibility that GDC gene transcription starts at multiple sites (cf. Gustincich et al., 2006). Transcription start site determination and comparison of GDC cDNA sequence with genomic sequences of the clones shown in Fig. 1A revealed that this gene has 25 exons comprising 3572 bases in a 40-kb-long genomic region (Fig. 1A and Table 1). In a 7.5-kb-long region flanking the 5′-end of exon 1, KpnI

Table 2
Identification of the proximal promoter and its important *cis*-elements

Experiment 1		Experiment 2[a]				
Genomic region	Relative luciferase activity	Genomic region	Binding site	Name	Mutant sequence	Relative luciferase activity
−7500/+22[b]	40.7±6.0	−107/+22	CP2	WT	-16 CCGCGCCGCACCGC -3	33.0±3.4
−4155/+22	27.3±2.3			M1	-16 ACGTGCCGCACCGC -3	36.6±3.6
−2113/+22	37.5±6.3			M2	-16 CCGCGCCGCAACGT -3	26.1±2.4
−1518/+22	32.4±9.9			M3	-16 CCGCGCCGCAACAT -3	28.7±2.4
−520/+22	39.0±7.8			M4	-16 ACATGCCGCAACAT -3	16.4±1.3
−107/+22	25.9±4.6					
−7500/−108	1.0±0.1		NF-Y/CP2	WT	-36 ATTGGCGCTGG -26	33.0±3.4
				M5	-36 AATTCCGCTGG -26	29.4±9.7
−82/+22	19.7±3.5			M6	-36 ATTGGCGATGT -26	31.8±9.8
−56/+22	8.0±1.7					
−35/+22	1.2±0.3		UpSp1	WT	-71 GAGGCGGGGC -62	33.0±3.4
				M7	-71 GATTCGGGGC -62	7.5±0.1
pGL-3B[c]	1.0			M8	-71 GAGGCTA TAGGC -62	18.3±1.8
		−56/+22	InvSp1	WT	-54 GCACCGCCTC -45	33.0±3.4
				M9	-54 GCACCGAATC -45	20.7±2.6
			InvSp1	WT	-54 GCACCGCCTC -45	7.5±1.3
				M10	-54 GCACCGAATC -45	5.1±1.4

[a] −107/+22 and −56/+22 with mutagenized nucleotides (underlined) were defined as M1 to M10 and assayed for promoter activity. Relative luciferase activity was expressed as mean value±SD of four assays.

[b] In Experiment 1 and 2, promoter assay was performed using genomic regions prepared at the recognition sites for BamHI (−7500), downstream KpnI (−4155), upstream XbaI (−2113), EcoRI (−1518), PstI (−520), SalI (−107) and artificial XhoI (+22). Their relative positions are also shown with nucleotide numbering in Fig. 1B.

[c] pGL-3 basic vector.

(−4155), XbaI (−2113), EcoRI (−1518), PstI (−520) and SalI (−107) mapped their recognition sites, and base sequencing confirmed them at the parenthesized positions (Fig. 1B). The 5′-end BamHI site and the upstream KpnI site were mapped by electrophoresis at positions −7.5 and −6.9 kb distant from the major transcription start site (Fig. 1B). A nucleotide sequence including regions required for transcription regulation is shown in Fig. 1D. The codon for the active-site lysine residue (738K) of GDC resides in exon 19. Exon/intron boundaries of the chicken GDC gene resemble those of the human GDC gene, although the transcription start site of the chicken GDC gene differs by the definition adopted in structural analyses of the human GDC gene (Takayanagi et al., 2000).

3.2. The chicken GDC gene locus

Taking advantage of use of the AB245436 and NM_204322 for chicken GDC gene locus identification, we tried to align segments from the two sequences over chicken genomic DNA sequences. Blat analyses respectively assigned the first base of AB245436 (the first nucleotide of KpnI site at −4155) and the 3499th T immediately upstream from the first adenine base of poly(A) tail in the chicken GDC cDNA sequence in NM_204322 (the 3′-end of exon 25) to the bases at 28600582 and 28557830 in the chicken chromosome Z minus strand. However, a 3′-region of the AB245436 sequence and regions upstream from the 5′-end of exon 3 appeared to be defective in the UCSC database sequence. Another chicken chromosome Z sequence (accession number: AC202790) in High-Throughput Genomic Sequence Database (http://www.ncbi.nlm.nih.gov/HTGS/) had the defective region. In the AC202790 sequence, the 5′-end of the AB245436 sequence and the 3′-end of exon 25 corresponded to 198347 and 240569, encompassing a 42,222-base-long region in which there were 25 exonic sequences with the 5′- and 3′-ends basically similar to those shown in Table 1. Thus, the chicken GDC gene locus may reside in the chromosome Z minus strand. Database searches revealed that the entire sequences of UpR1S+UpR1A and UpR2S+UpR2A reside only in the chicken GDC gene locus. A segment −324/−302 of UpR1A is included in chicken chromosome 2 DNA as a coding region of an mRNA sequence (XM_418505). Similar region (−321 to −302) was present in chromosome 5 DNA (56222862–56222881). Concerning the ENSGALG00000015053 related sequence, exons 1 and 2 of the GCSP gene begin at positions near 5′-ends of the true exons 3 and 4 yielding a reading frame quite different from that in NM_204322.

3.3. Chicken GDC gene promoter

Serial deletion mutants of the 7.5-kb flanking region were unidirectionally prepared as regions between one of the six native cleavage sites by the restriction enzymes listed above and the artificial XhoI site at +22. These genomic regions were defined as −7500/+22, −4155/+22, −2113/+22, −1518/+22, −520/+22 and −107/+22 (Fig. 1B and Table 2) and ligated upstream from a reporter firefly luciferase gene in a pGL3-basic vector to assay for promoter activity in recipient LMH cells which had GDC mRNA at about 10% of its hepatic level in the adult chicken (lane L of the left panel in Fig. 2B). The cells transfected with one of the six constructs showed luciferase activity ranging from 26 to 40 in arbitrary units (Experiment 1 in Table 2). The −7500/−108 region that is identical to the pBS insert (see Materials and methods) was inactive, indicating that the proximal −107/+22 region is required for luciferase gene transcription. The most downstream region, −82/+22, which significantly increased luciferase activity (Experiment 1 in Table 2) was GC-rich (14 CpG pairs among 34C and 35G nucleotides within the −82/−1 region) and had neither a canonical TATA box (Breathnach and Chambon, 1981; Maniatis et al., 1987) nor an initiator sequence (Corden et al., 1980; Smale and Baltimore, 1989) (Fig. 1C and D). Instead, this region had several binding motifs for the following known *trans*-activators: upstream Sp1 (−71 to −62, UpSp1) and inverted Sp1 (−54 to −45, InvSp1) (Dynan and Tjian, 1983), NF-Y (−36 to −32, ATTGG) (Chodosh et al., 1988; Mantovani et al., 1992; van Huijsduijnen et al., 1990), and CP2 (−29 to −26 as CNRG, and −16 to −3 as CNRGN6CNRG) (Lim et al., 1993; Murata et al., 1998). The −82/+22, −56/+22, and −35/+22 regions, which are three serial deletion mutants of UpSp1, InvSp1 and part of the NF-Y motif, respectively exhibited 80%, 30% and 3% of luciferase activity exhibited by −107/+22.

3.4. Functional confirmation of the putative cis-elements

Experiment 2 in Table 2 summarizes results from functional examinations of pGL3-based constructs each carrying one or more motifs mutagenized in −107/+22 and −56/+22. The downstream CP2 motif with increasing numbers of base substitutions up to 6 bases (M1 to M4) decreased luciferase activity to 50% of that yielded by the wild-type −107/+22. Mutations in the NF-Y/CP2 motif were ineffective on promoter activity (M5 and M6). M7 with mutations in UpSp1 in −107/+22 lost 80% of the activity of the wild-type sequence. M8 with substitutions at different positions in UpSp1 of −107/+22 (GG at −66 and −65 to TA), and M9 with comparable mutations in InvSp1 in −107/

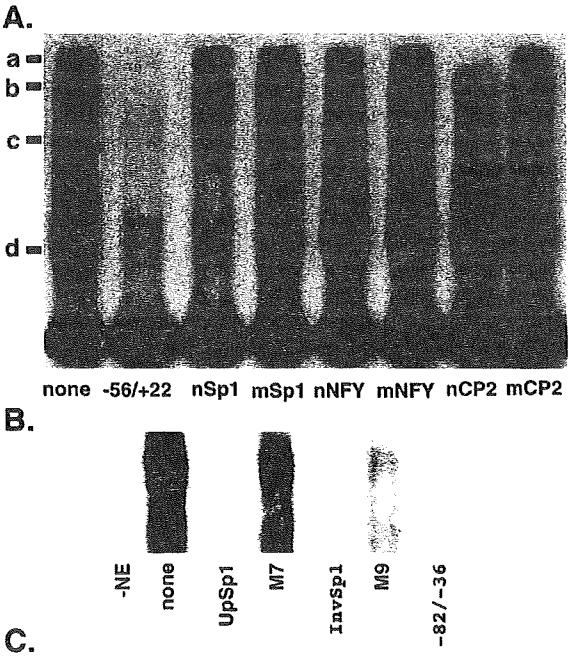

Competitor	Nucleotide sequence
nSp1	5′-ATTCGATCGGGGCGGGGCGAGC-3′
mSp1	5′-ATTCGATCGGTTCGGGGCGAGC-3′
nCP2	5′-AGCTGACCAGTTCCAGCCACTCTTTAGTC-3′
mCP2	5′-AGCTGAACATTTACATACACTCTTTAGTC-3′
nNF-Y	5′-GATCCCTTTTAACCAATCAGAAAAATGTG-3′
mNF-Y	5′-GATCCCTTTTAAGAATTCAGAAAAATGTG-3′
UpSp1	−82 CAGGTGGCGGCGAGGCGGGGCGAGCG −57
M7	−77 GGCGGCGATTCGGGGCGAGC −58
InvSp1	−36 GGGGAGGAGAGGCGGTGCCG −56
M9	−36 GGGGAGGAGATTCGGTGCCG −56

Fig. 3. Binding of proteins to the promoter. (A) EMSA using [^{32}P]-labeled −56/+22 and chicken liver nuclear extracts (10 μg). Letters a, b, c, and d verify major bands. Competitors are shown under each lane. (B) EMSA using −82/−57 probe. Conditions are similar to those used in (A). (C) Competitors used in (A) and (B). Motifs and mutagenized bases in native (n) and mutant (m) competitor sequences are underlined.

+22 were respectively 50% and 60% as active as the wild-type sequence. M10 prepared by introducing the mutations identical to those in InvSp1 of M9 into −56/+22 was 65% as active as the wild-type −56/+22, implying that UpSp1, InvSp1 and the downstream CP2 motifs are required for transcription activity.

3.5. The binding of proteins to the cis-elements

EMSA using liver nuclear extracts of chickens at 4 months of age and a [^{32}P]-labeled −56/+22 probe revealed four bands defined as a, b, c and d (Fig. 3A, lane "none" indicating none of the competitors), all of which were abrogated with the cold −56/+22 competitor (Fig. 3A, lane −56/+22). Native competitors for CP2 (lane nCP2), NF-Y (lane nNFY) and Sp1 (lane nSp1) respectively abrogated the bands a, b and d. Data indicate that InvSp1 actually binds an Sp1-like protein. The −82/−57 probe in which UpSp1 is present (Figs. 1C and 3C) yielded bands that were abrogated with both UpSp1 and InvSp1 competitors, whereas their mutants, M7 and M9, did not completely abrogated them (Fig. 3B). Therefore, UpSp1 is likely to be a binding site for an Sp1-like protein. The NF-Y/CP2 motifs formed DNA/protein complex (Fig. 3A), although their mutagenized motifs did not appear to clearly affect promoter activity (Table 2). Properties of band c are unclear at present, since it disappeared in response to mSp1 and mCP2 (Fig. 3A). We further tried to confirm immunochemical properties of the *trans*-factors. Western blot analysis, however, revealed that commercially available antibodies each specific to rodent Sp1, C/EBP-α and β and NF-Y were unreactive to chicken liver nuclear proteins. Taking the properties determined by promoter assays and EMSA into account, we assigned −82/+22 to the proximal promoter of the chicken GDC gene. As estimated by the difference in activity of −107/+22 from that of −82/+22 in Experiment 1 of Table 2, the −107/−83 region was thought to have an element that increases promoter activity.

3.6. Changes in promoter activity by upstream regions

To address whether the cloned 5′-flanking region has additional regions that change promoter activity, LMH cells were transfected with constructs in which appropriately cleaved 5′-flanking regions were directly ligated to −107/+22 (Fig. 4A). Of these, a construct carrying a region between a KpnI site at −4155 and an XbaI site at −2113 (we defined this region as KX) clearly increased luciferase activity in LMH cells (construct 4 in Fig. 4A), indicating that KX and −2113/−83 may have regions that change promoter activity. Actually, −520/−108 appeared to suppress the KX-dependent promoter activation (constructs 2 and 3 in Fig. 4B). Sequential removal of short segments within this region in the 5′ to 3′ direction, however, changed promoter activity in a somewhat more complicated manner as follows; in Fig. 4C, KX activity is detectable in the presence of −345/−292 (construct 4) and −107/+22 (construct 8), whereas

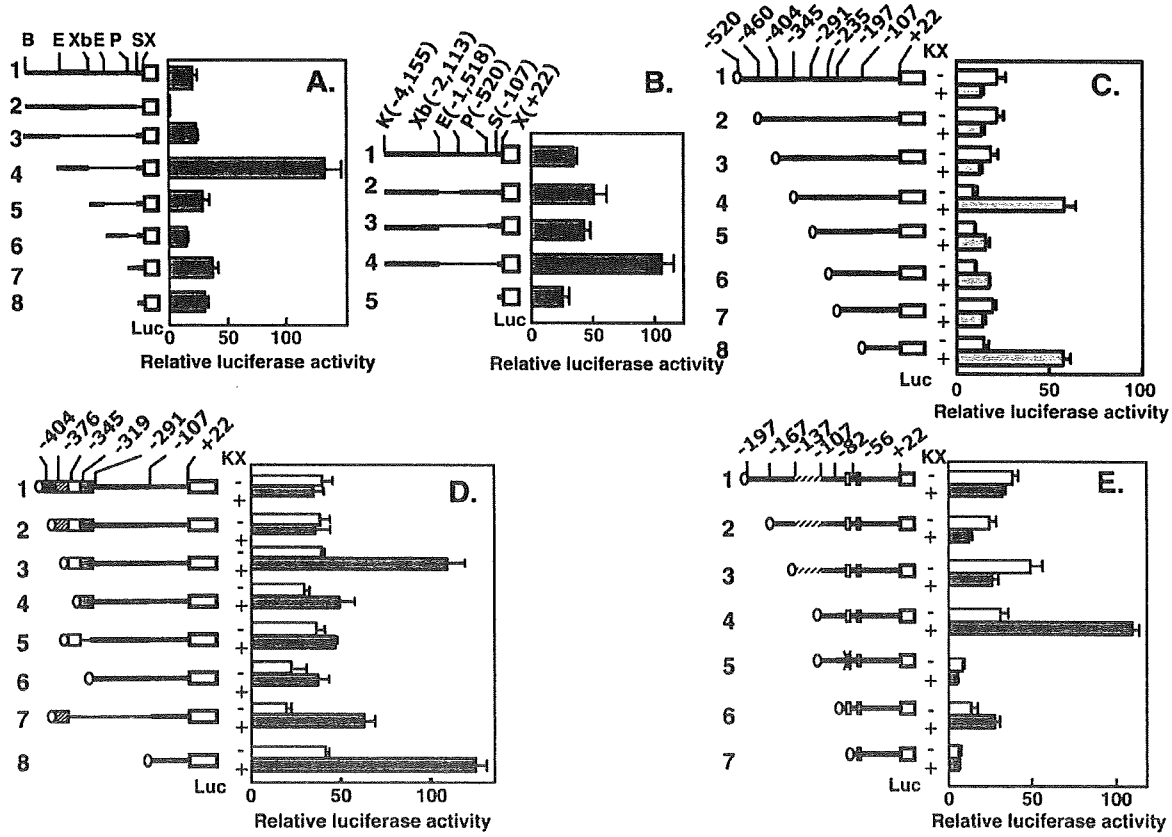

Fig. 4. KX-dependent promoter activation and its suppression by four UpRs. (A) Activation of the promoter by KX. The numbering verifies pGL3-basic vector-based constructs. The 5′-flanking region (bold line) was cut at sites shown over construct 1 (initials in uppercase letters). Various regions were ligated at the 5′-end of −107/+22 in a pGL3-basic vector to assay for promoter activity in LMH cells. (Luc) and (open box) denote a luciferase gene. Note that −107/+22 had been deleted in construct 2. (B) Regions that change promoter activity. −4155/−2113 (KX) was ligated to the 5′-ends of serial deletion mutants of the 5′-flanking region (bold line) at EcoRI (E), PstI (P) and SalI (S) sites and assayed for promoter activity. Precise lengths of the insert in (A) and (B) can be calculated by parenthesized nucleotide numbering. (C) to (E) Identification of the UpRs. Promoter activity was assayed using various deletion mutants of the genomic region from −520 to −56 with (+, filled bar) or without (−, open bar) ligation of KX (oval symbol). Small rectangles in (E) denote UpSp1 and InvSp1 and a mutant UpSp1 with X. Thin lines in (A), (B) and (D) denote regions skipped by deletion.

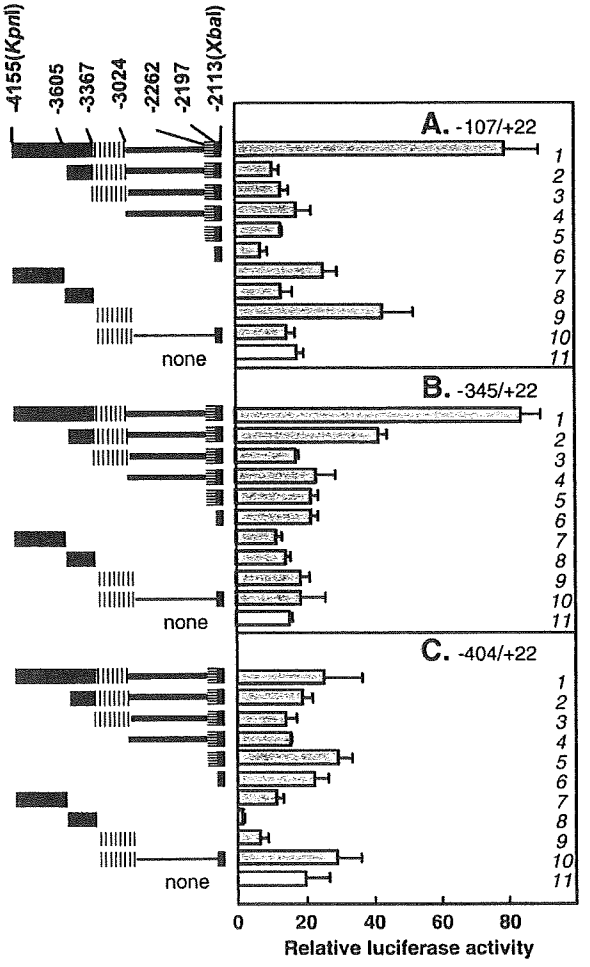

Fig. 5. The potential of segments within KX to change promoter activity with the aid of UpRs. Indicated segments of KX were ligated to 5′-ends of −107/+22 (A), −345/+22 (B), and −404/+22 (C) and assayed for promoter activity in LMH cells. None denotes the recipient DNA alone. Thin lines are the skipped genomic regions. Constructs are verified by the numbering.

the KX-dependent promoter activation was suppressed in the presence of −376/−346 (construct 2 in Fig. 4D) and −137/−108 (construct 3 in Fig. 4E).

3.7. KX-dependent regulator regions

−376/−346 may have suppressor activity, since KX activates the promoter by the removal of −376/−346 (Fig. 4D, constructs 1, 2 and 3). −345/−291 may have an activator whose activity is lost by the cleavage at −319 (Fig. 4D, constructs 3, 4 and 5). The consecutive −376/−346 and −345/−291 regions were thus designated *up*stream regulator region *1* for suppression and *a*ctivation of transcription (UpR1S and UpR1A). Additional suppressor activity was detectable in −137/−108 (Fig. 4E, constructs 3 and 4). −107/−83 by itself slightly increases promoter activity of −82/+22 as −107/+22 (Table 2, Experiment 1 and open bars of constructs 4 and 6 in Fig. 4E). Moreover, −107/−83 appeared to KX-dependently activate the promoter (Fig. 4E, constructs 4 and 6). Therefore, −137/−108 and −107/−83 regions were designated UpR2S and UpR2A. Each UpR appears to abolish the function of an immediately downstream UpR in a hierarchical manner in LMH cells. While −82/+22 was weakly responsible to KX, −56/+22 without UpSp1 was not (Fig. 4E, constructs 6 and 7). −107/+22 with the mutant UpSp1 (M7) was also insufficient to respond to KX (Fig. 4E, constructs 4 and 5). UpSp1 thus appears to be important to the KX-dependent promoter activation.

3.8. Interaction of segments within KX with UpRs

Various fragments derived from KX were ligated to 5′-ends of −107/+22, −345/+22, or −404/+22, which respectively have UpR2A (Fig. 5A), UpR1A, UpR2S and UpR2A (Fig. 5B), and the four UpRs (Fig. 5C). In Fig. 5A, the deletion of −4155/−3605 nullified the promoter activation by UpR2A (constructs 1 and 2). Conversely, −4155/−3605 and −3366/−3024 slightly increased promoter activity by direct ligation to −107/+22 (constructs 7 and 9). A short 3′-end fragment (−2197/−2113) decreased promoter activity of −107/+22 itself (construct 6) and cancelled the promoter activation in −107/+22 by −3366/−3024 (constructs 9 and 10). In Fig. 5B, the deletion of −4155/−3605 from KX (construct 2) decreased the promoter activation to 50% of that by the entire KX (construct 1). Other constructs did not show clear changes in promoter activity, indicating that the three UpRs interact with the promoter in a manner different from that of UpR2A alone. In Fig. 5C, addition of UpR1S to the three UpRs suppressed the promoter (construct 1). Of the fragments from KX, −3604/−3367 strongly and −3366/−3024 weakly suppressed the promoter in the presence of the four UpRs (constructs 8 and 9). Notably, further insertion of −2197/−2113 into the construct 9 abolished this suppression (construct 10). In summary, −4155/−3605 was involved in the promoter activation and −3604/−3367 appeared to suppress it. −3366/−3024 appeared to function in both the promoter activation and its suppression. −2197/−2113 restored promoter activity changed by −3366/−3024 to the basal activity (constructs 9 and 10 in Fig. 5A and C). Conclusively, the four segments within KX participate in the regulation of promoter activity.

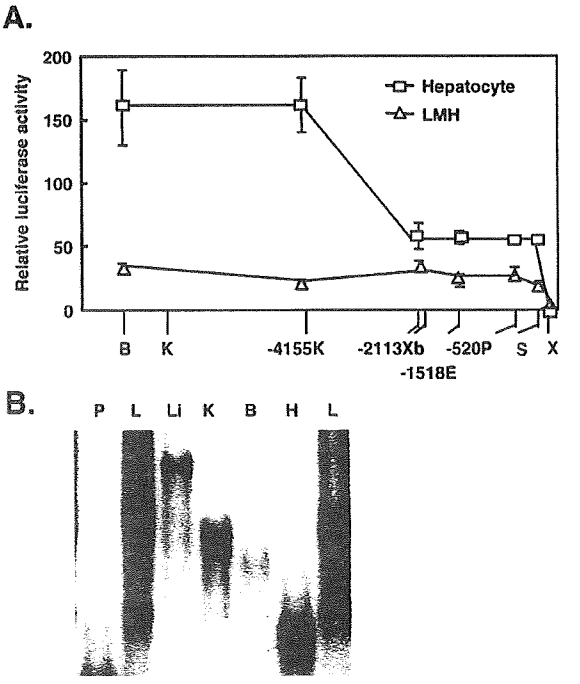

Fig. 6. Cell-type specific functions of KX and UpRs. (A) Recombinant plasmids used in Experiment 1 in Table 2 were assayed for promoter activity in hepatocytes in primary culture (open square) and LMH cells (open triangle). B, K, Xb, E, P, S and X indicate positions used for preparation of serial deletion mutants (see Fig. 1B). (B) EMSA using [^{32}P]-labeled UpR2A (−107/−83) probe and nuclear extracts from LMH cells (lanes L), liver (lane Li), kidney (lane K), brain (lane B) and heart (lane H) from chickens at 4 months of age. Probe alone was loaded onto lane P.

3.9. Cell-type specific regulation of the promoter

To address whether KX similarly functions in hepatocytes and LMH cells, the serial deletion mutants used in Experiment 1 of Table 2 were assayed for luciferase gene expression in hepatocytes in primary culture. Of the six mutants tested, the two constructs with KX (constructs having genomic regions upstream from −2113) increased luciferase activity in hepatocytes to a level 3-fold higher than those expressed by constructs without KX (Fig. 6A). LMH cells, when transfected with identical sets of the plasmids, did not exhibit the KX-dependent change in promoter activity (Experiment 1 in Table 2, and Fig. 6A). Moreover, the constructs without KX yielded higher levels of luciferase in hepatocytes than in LMH cells. These findings support the possibility that UpR1S and UpR2S are at least less active in hepatocytes than in LMH cells probably in a cell-type specific manner.

3.10. Proteins binding to UpR2A

To gain more insight into tissue-specific functions of UpRs, UpR2A (−107/−83) was examined for properties in binding protein (s). EMSA using a [^{32}P]-UpR2A probe revealed that nuclear extracts from the liver, kidney, and brain from chickens at 4 months of age had UpR2A binding proteins that respectively yield a single, clear signal but with mobility intrinsic to each tissue (Fig. 6B, lanes Li, K and B). Nuclear extracts from the heart, which lacks GDC, gave a signal with faster mobility than those revealed for other tissues (Fig. 6B, lane H). LMH cell nuclear extracts yielded signals whose number and mobility differ from those given by the four tissues (Fig. 6B, lanes L). Despite the presence or absence of GDC, the adult chicken tissues likely have UpR2A binding proteins in different populations.

3.11. Putative cis-element in UpR2A

UpR2A was examined by similar procedures for a putative segment to which nuclear proteins can bind. For this purpose, mutant UpR2A competitors were prepared by substitutions of three consecutive nucleotides in every 3-nucleotide interval (Fig. 7A). A wild-type [^{32}P]-UpR2A probe incubated with liver nuclear extracts from chickens at 4 months of age formed a signal similar to that in lane Li in Fig. 6B (Fig. 7B, lane N+, C−). Prior incubation of the nuclear extract with 200-fold molar excess wild-type UpR2A competitor abrogated this signal (lane WT), indicating the binding of protein(s) to particular sequences of UpR2A. This signal was detectable even after prior incubation of the nuclear extract with an M12 mutant competitor (Fig. 7B, lane M12). M14 and M16 competitors also yielded weak signals with a slightly larger mobility than those in lanes N+, C− and M12 (Fig. 7B, lanes M14 and M16). These findings indicate that UpR2A interacts with liver nuclear proteins in a sequence encompassing −104 to −90. In competition with M12, LMH cell nuclear extracts yielded a weak signal with mobility similar to those found in lanes N+, C− and M12 in Fig. 7B (Fig. 7C). Therefore, LMH cells have UpR2A binding proteins similar to those in the liver but in a lesser amount, compared to their hepatic level.

3.12. UpR2A mutants in the KX-dependent promoter activation

We respectively inserted the mutant UpR2A sequences between KX and the promoter region (−82/+22) in pGL3-basic vectors and

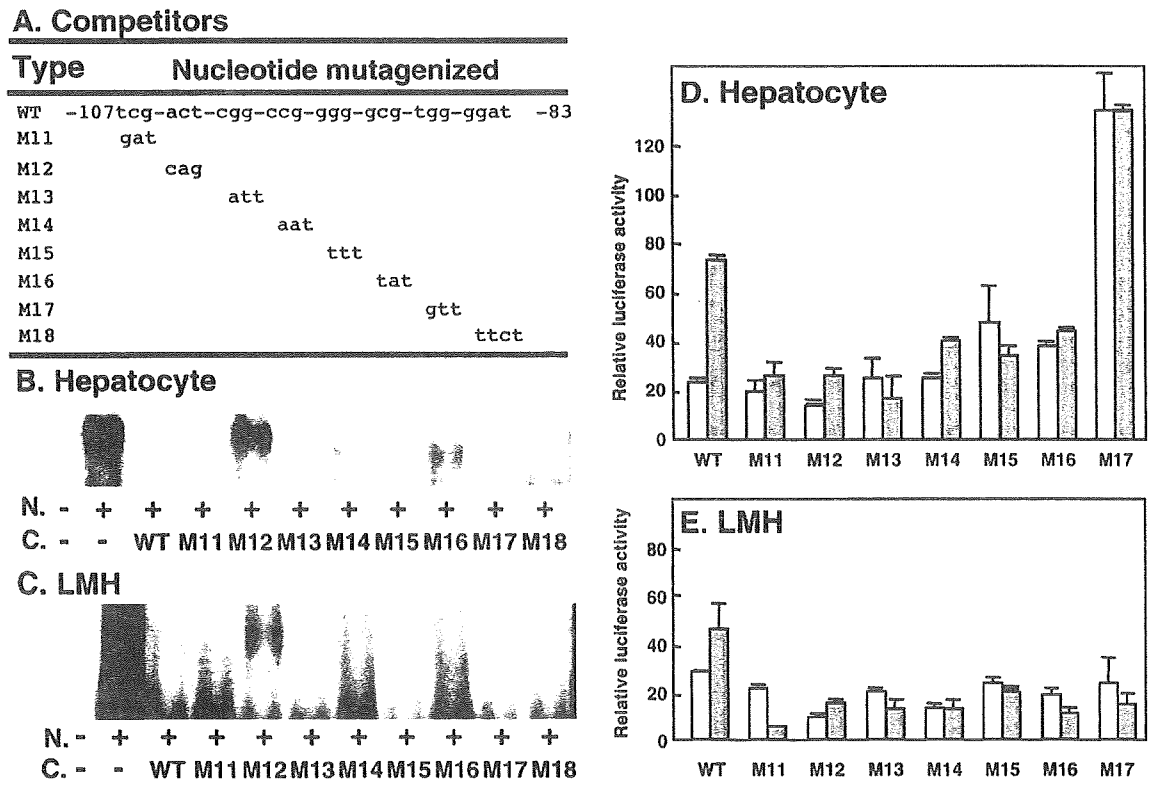

Fig. 7. Binding of nuclear proteins to UpR2A. (A) Structures of wild-type and mutant UpR2A. Three bases mutagenized in mutant UpR2A (M11 to M18) are shown at the corresponding positions along with the wild-type (WT) sequence. (B) and (C) EMSA using [^{32}P]-labeled WT UpR2A probe and wild-type and mutant competitors (WT and M11 to M18 under the panels). Liver nuclear extracts from chickens at 4 months of age and LMH cell nuclear extracts were used in (B) and (C). N and C stand for the nuclear extracts and competitors. (D) and (E) −107/+22 with either WT or M11 to M17 UpR2A were constructed in pGL3-basic vectors and assayed for the promoter activation with (filled bar) or without (open bar) ligation of KX in hepatocytes in (D) and in LMH cells in (E). Control cells were transfected with empty vector.

compared extents of the KX-dependent promoter activation by the mutants with those by wild-type UpR2A in hepatocytes and LMH cells (Fig. 7D and E). In hepatocytes, the wild-type UpR2A construct clearly increases promoter activity (Fig. 7D, filled bar for WT) in a KX-dependent manner to a larger extent than that in LMH cells (Fig. 7E, filled bar for WT). The mutant constructs were defective in the KX-dependency in the promoter activation (Fig. 7D, filled and open bar). Therefore, the binding of nuclear proteins to a segment from −104 to −90 is indispensable to the KX-dependent promoter activation. The M17 construct exhibited extraordinarily high promoter activity, with or without KX, in a manner intrinsic to hepatocytes, although the mechanisms are unclear at present.

3.13. UpR-like sequences around the 5′-end of exon 1 of the human GDC gene

We have shown that regulator regions with the illustrated location (Fig. 8A) are required for chicken GDC gene transcription. The UpR1 and UpR2 sequences do not appear to be highly similar (Fig. 8B). Taking advantage of this feature, we examined whether 5′-flanking and 5′-untranslated regions of the human GDC gene possess regions similar to the chicken UpR1S/UpR1A and UpR2S/UpR2A sequences (Fig. 8C), since chicken and human GDC genes resemble in many respects (Kume et al., 1991; Takayanagi et al., 2000). In this comparison, there were several problems resulting from incorrect understanding of general gene structures by Kure and colleagues (Takayanagi et al., 2000). For example, despite the finding that transcription of the human GDC gene probably begins with the guanine base 163 bases upstream from the adenine base of the translation start codon, the authors confusedly assigned this adenine base to the 5′-end of exon 1 in Table 2 and Fig. 3 (Takayanagi et al., 2000). In this context, we have reported that the human GDC cDNA had a 5′-untranslated sequence comprising 150 bases (Kume et al., 1991). This untranslated sequence is entirely included in the human genomic sequence from −150 to −1 in Fig. 3B by Takayanagi et al. (2000). Therefore, in the present paper, we defined the guanine nucleotide at −163 as a putative 5′-end of exon 1 of the human GDC gene. This definition is extremely important, since human genomic DNA sequences similar to those of UpR1 and UpR2 were found respectively in the 5′-flanking region and in the 5′-untranslated region (Fig. 8C). Notably, the UpR2A segments mutagenized for M12, M14, and M16 preparation appeared to be conserved in the human genomic DNA sequence. The KX segments were not compared with the human DNA sequence, since those are still too long to be used for the comparison.

3.14. Chicken UpR-related sequences in the human genome

The human genome had 19 UpR1- and 7 UpR2-related sequences (Figs. 9 and 10). This suggested and actual comparison of the human and chicken sequences confirmed that the UpR sequences are in part conserved together with binding motifs for transcription factors. The 14 UpR1A-related sequences that resemble the −347/−327 segment (sequence in red) of UpR1A represent the conserved sequence (Fig. 9). This UpR1A region included motifs for YY1 (arrows 1 and 2), δ Factor (a homologue of YY1, arrow 3), repressor of CAR1 expression (arrow 4), T-Ag (arrow 5), RXR and T3R (arrow 6), AML1 (arrow 7), AP-2 (arrow 8) and TCF-4E (arrow 9). These motifs are conserved in most human

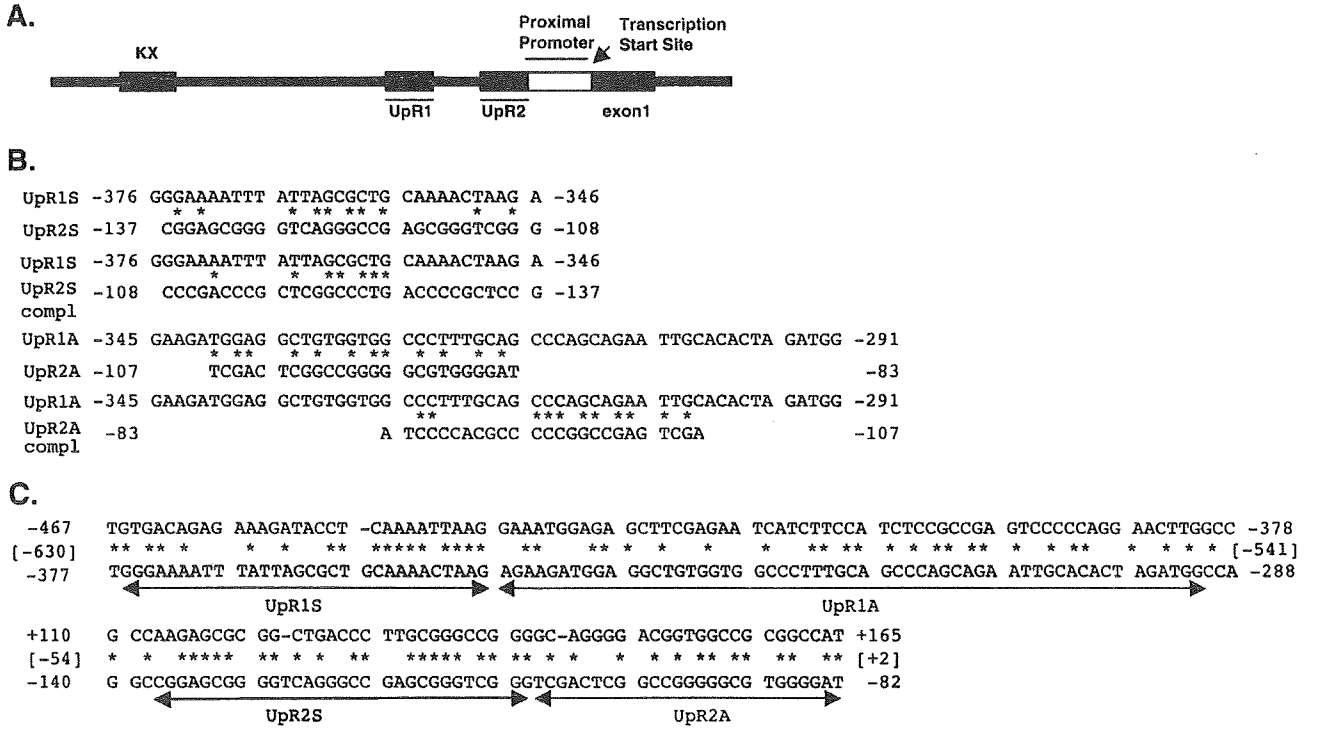

Fig. 8. Genomic regulator regions. (A) Schematic illustration of the chicken KX (red), UpR1S and UpR2S (blue), UpR1A and UpR2A (red), proximal promoter (open bar), and exon 1 (green). (B) Sequence similarity of UpR1S and UpR1A to UpR2S and UpR2A. Identical bases were indicated with asterisks. "Compl" denotes complementary sequence. (C) The human genomic DNA sequences similar to chicken UpR1S/UpR1A and UpR2S/UpR2A. Chicken UpR1S+UpR1A and UpR2S+UpR2A were aligned over 5′-flanking and 5′-untranslated regions of the human GDC gene, respectively. Arrows indicated genomic regions of UpR1S and UpR2S (blue) and UpR1A and UpR2A (red). Based on our conclusion that −163 described by Takayanagi et al. (2000) is the putative transcription start site and +1, the numbering is shown without parenthesis and instead, the numbering by Takayanagi et al. (2000) is parenthesized for human genomic sequences.

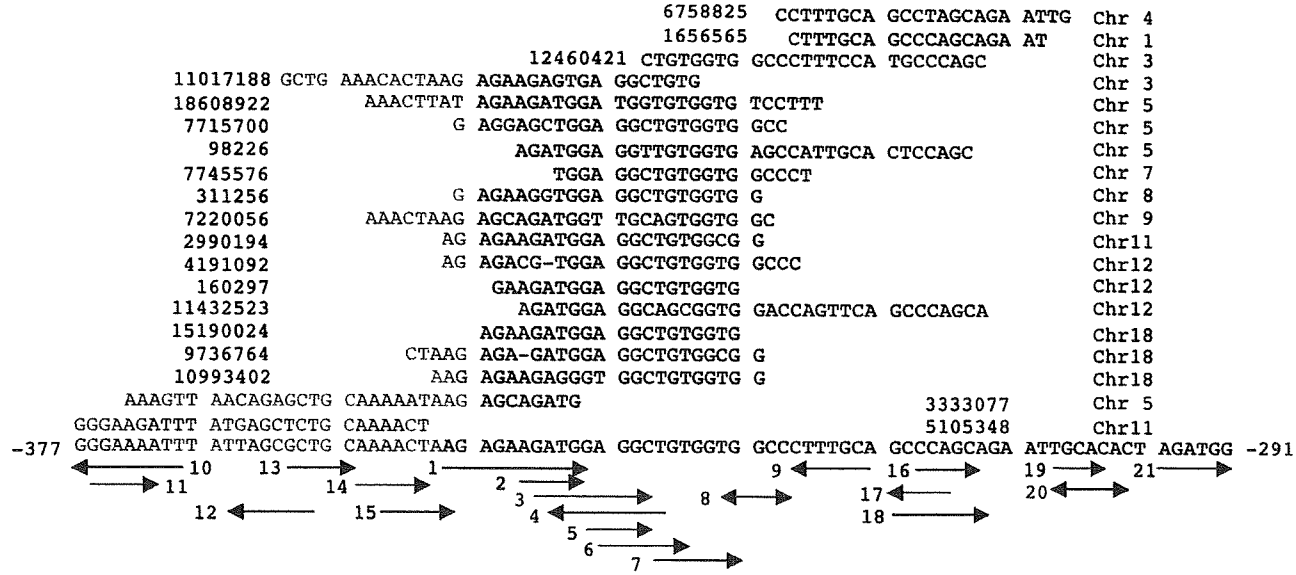

Fig. 9. Human genomic DNA similar to UpR1S+UpR1A. Human genome databases were examined for sequences similar to UpR1S+UpR1A using Blat at UCSC and Blast at NCBI. Chicken UpR1 sequence were examined for transcription factor binding motifs by Patch at Gene-regulation. com (http://www.gene-regulation.com/). Arrows indicate positions of predicted motifs. In the bottom row, UpR1S and UpR1A are shown in gray and black. The region indicated in red is the region most prevalent in the human genome. Human DNA sequences similar to part of UpR1 sequence were shown together with chromosome number and nucleotide position at one end.

DNA regions. UpR1S shown in gray had motifs for C/EBP isoforms (arrow 10), ICGF-3 and NFAT isoforms (arrow 11), E2F isoforms (arrow 12), CTCF (arrow 13), AR (arrow 14) and HNF-4α (arrow 15). The 3′ half of UpR1A had motifs for LBP-1 (arrow 16), T-Ag (arrow 17), AP-2 (arrow 18), Sp1 (arrow 19), GR and MTF-1 (arrow 20), and YY1 (arrow 21). Fig. 10 indicates that most human sequences conserved correspond to UpR2S sequence. In UpR2S, motifs for YY1 (arrow 1), GAGA factor (arrows 2 and 6), LMC (arrow 3), FXR and RXR (arrow 4), AP-1, T3R, COUP and RAR (arrow 5 and 7) are present. In UpR2A, those for ARP-1 (arrow 8), PAI-2 (arrow 9), Glob-B (arrow 10), AP-2 and HNF-3 (arrow 11), C-ACT (arrow 12), T-Ag (arrow 13), AhR and Arnt (arrow 14) and AP-2, MBP-1, and NFκB (arrow 15) are present. Of 7 human chromosomes, chromosome 15 had a sequence similar (76%) to a segment from −136 to −84 of UpR2 with 1 gap together with motifs shown with arrows 1 to 3, 6 and 8. This begins 70 bases upstream from the transcription start site of the human cellular retinoic acid binding protein gene. Chromosome 19 DNA had −140/−114 of UpR2S as the +40/+66 region of the human intron-less Jun D proto-oncogene. These regions might function in the regulation of transcription and translation. A motif (−104/−97, arrow 10) for Glob-B (a transactivator of β-globin locus control region) (Walters et al., 1991), which is an LSF/Grainyhead transcription factor family member (Venkatesan et al., 2003), notably encompasses the M12 region (−104/−102). Another family member might bind to this motif in hepatocytes. Motifs for YY1 and CTCF, which are known as a silencer or an insulator (Baniahmad et al., 1990; Shirra and Hansen, 1998; Fourel et al., 2002; West et al., 2002; Kim et al., 2003), are present together with that for δ factor (a homolog of YY1) in a UpR1S/UpR1A boundary region. YY1 sites are also present in the 3′-end of UpR1A and in UpR2S, suggesting that these factors function in the suppression of the GDC gene promoter.

4. Discussion

The present study has clarified for the first time several structural and functional characteristics involved in the regulation of vertebrate GDC gene transcription. The chicken GDC gene comprises 25 exons with the entire sequence of 3572 bases in the region between 202,503 and 240,569 on the chromosome Z minus strand (accession number: AC202790) and encodes the active site lysine residue in exon 19. −82/+22, which has binding motifs similar to those for the known Sp1, NF-Y and CP2, is absolutely required for promoter activity. All the *cis*-elements bind nuclear proteins. UpSp1, InvSp1 and the downstream CP2 motifs are indispensable for promoter activity. Thus, we assigned −82/+22 to the chicken GDC gene proximal promoter.

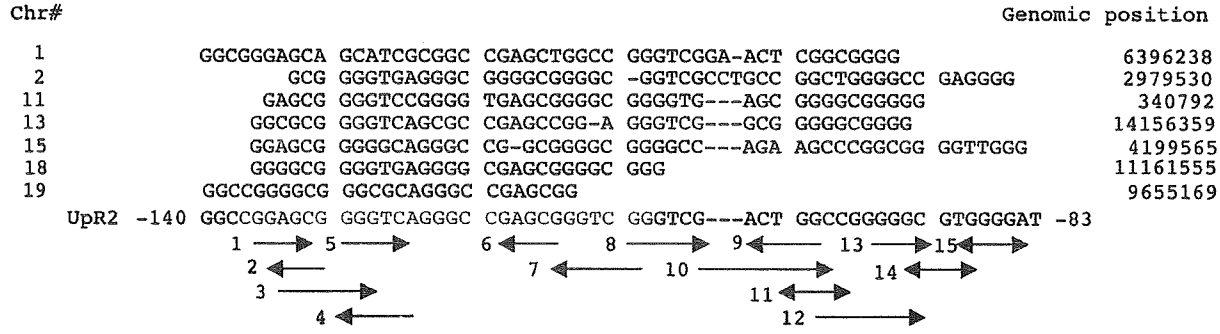

Fig. 10. Human genomic DNA similar to UpR2S+UpR2A. Human genomic sequences were selected and analyzed by the procedures similar to those used in Fig. 9. UpR2S and UpR2A are shown in gray and black, respectively.

Promoter assays in LMH cells and hepatocytes have clarified that a 5′-flanking region from −4155 to −83 encompasses KX, UpR1S, UpR1A, UpR2S and UpR2A regions that may change promoter activity. −4155/−3605, −3604/−3367, −3366/−3024 and −2197/−2113 within KX appeared to have the potential to interact with different UpR counterparts, since these segments in KX activate, suppress or restore promoter activity in various types of recombinant constructs in which KX coexists with one to four UpRs and the proximal promoter (Fig. 5). In the promoter, UpSp1 (−71 to −62), which is the most upstream element, is 12 bases downstream from UpR2A. A −107/+22 construct with a mutagenized UpSp1 (M7 in Table 2 and construct 5 in Fig. 4E) largely lost both the promoter activity and the potential to respond to KX and UpR2A in the promoter activation. The native genomic organization of the four regions in KX, the four UpRs and the elements in the proximal promoter is thought to be prerequisite for their cooperation in chicken GDC gene transcription regulation.

Taking general mechanisms of transcription regulation into account, it is likely that these genomic regions recruit proteins to accomplish the regulation. Actually, in UpR2A, the −104/−102 segment is indispensable to bind liver nuclear protein(s). The Glob-B binding motif, GACTGGC (Walters et al., 1991), encompasses this segment. Proteins recognize the motif might play a principal role in the promoter activation. Low sequence similarity of the four UpRs suggested different categories of the functions of the UpRs. Actually, this was emphasized by the finding that transcription factors predicted likely assign UpR1S and UpR2S to suppressor or insulator and UpR1A and UpR2A to enhancer. Molecular characterization of the binding proteins would clarify roles of the four UpRs in GDC gene transcription.

On the genomic DNA stretch, UpR2S and UpR2A can be localized on an identical nucleosome together with the proximal promoter. UpR1S and UpR1A may be located on the adjacent nucleosome, whereas the segments in KX are estimated to be 15 to 30 nucleosomes distant from the 5′-end of UpR2A. Therefore, mechanisms by which particular regions in KX are placed in proximity to the promoter are thought to be most important in the regulation of GDC gene transcription. Looping of the nucleosomal stretch is an attractive mechanism by which KX regulates promoter activity with the aid of the four UpRs. Histone modification by acetylation (Pazin and Kadonaga, 1997; Struhl, 1998; Bulger, 2005), methylation (Tachibana et al., 2002), phosphorylation (Pantazis et al., 1984), ADP-ribosylation (Kim et al., 2005), and sumoylation (Nathan et al., 2003) might mediate chromatin remodeling to recruit proteins that bind to KX and the UpRs. Covalent DNA modification such as DNA methylation is a critical mechanism for chromatin remodeling (Klose and Bird, 2006).

The chicken GDC gene promoter is GC-rich as described in Results. In mammals, Weber et al. (2007) classified GC-rich promoter into three categories: high-, low- and intermediate-CpG promoters (HCP, LCP and ICP) by measuring G, C and CpG contents. According to their equation, the chicken GDC gene promoter with 0.96 of the ratio belongs to HCP (the ratio>0.75). Unlike LCP, hypermethylation of which decreases transcription activity, HCP was mostly hypomethylated and active in transcription in mammalian somatic cells. In this context, chromosomes Z and W determine the sexuality as Z/Z for male and Z/W for female. In humans, DNA methylation is involved in embryonic development, genomic imprinting, and X-chromosome inactivation. If chicken cells mimic these events, the GDC gene promoter might be a target for such regulation during embryogenesis. In the combination of the various types of reactions for chromatin remodeling and the functions of the four UpRs, chicken cells can determine GDC levels intrinsic to individual cells.

In a physiological aspect, GDC expression plays a key role in determining tissue-specific distribution of glycine cleavage activity. Previously, we showed that different GDC levels in different tissues are predominantly determined at the level of GDC gene transcription (Kure et al., 1991a). In the present study, we found several lines of evidence related to cell-type specific expression of GDC: 1) Chicken GDC gene promoter (−82/+22) may change transcription activity with the aid of KX and UpRs (Fig. 4A to E). 2) GDC gene promoter activity exhibited by the entire 5′-flanking sequence changes in response to types of recipient cells such as hepatocytes and LMH cells probably due to differences in use of UpR1S and UpR2S (Fig. 6A). 3) A construct (KX/UpR2A/promoter) prepared by direct ligation of KX to −107/+22 exhibited promoter activity to different extents in hepatocytes and LMH cells (columns for WT in Fig. 7D and E). 4) UpR2A binding proteins are present in various tissues in different populations (Fig. 6B). These functional properties support the possibility that the KX-dependent and UpR-mediated regulation of GDC gene transcription is a principal mechanism of GDC expression intrinsic to particular types of cells. Accordingly, together with the mechanisms for chromatin remodeling, KX and the four UpRs and the promoter binding proteins are physiologically relevant to determine glycine catabolism in various chicken tissues at different ages.

The 5′-flanking region and the 5′-untranslated region of the human GDC gene had sequences similar to UpR1S/UpR1A and UpR2S/UpR2A, respectively (Fig. 8). It is likely that these regions are human versions of UpR1 and UpR2, although the human GDC gene promoter has never been characterized. Of the genes for the three intrinsic components of the glycine cleavage system, the GDC gene is most prevalently responsible for defective glycine cleavage activity in patients with nonketotic hyperglycinemia (Kume et al., 1988; Sakakibara et al., 1990; Kure et al., 1991a,b, 2006; Kanno et al., 2007). The deletion at 5′-regions of this gene has been assigned as a major cause of this disease (Sakakibara et al., 1990; Kanno et al., 2007). The present study suggested that the 5′-region of the chicken GDC gene by nature is likely flexible and mobile to accomplish the KX-dependent and UpR-mediated regulation. If the putative UpR1 and UpR2 segments similarly function in human cells, then the exonic sequence similar to UpR2S/UpR2A might confer the human GDC gene a complicated conformation in the course of the mutual conversion of the activated, suppressed and silenced conformations of the promoter at the initial stage of human reproduction including germ cell production. These physiological mechanisms might fortuitously be a cue for the pathological deletions of the human GDC gene. Molecular characterization of the KX-dependent and UpR-mediated regulation of the GDC gene promoter would help better understanding of the physiological and pathological implications of chicken and human GDC gene transcription. In future study, the UpR2A binding protein(s) that must interact with proteins binding to upstream and downstream elements should be initially identified to delineate the problem of interest.

Acknowledgement

This work was supported in part by a Grant-in-Aid (14370052) from the Ministry of Education, Culture, Sports, Science and Technology, Japan.

References

Baniahmad, A., Steiner, C., Kohne, A.C., Renkawitz, R., 1990. Modular structure of a chicken lysozyme silencer: involvement of an unusual thyroid hormone receptor binding site. Cell 61, 505–514.

Breathnach, R., Chambon, P., 1981. Organization and expression of eukaryotic split genes coding for proteins. Annu. Rev. Biochem. 50, 349–383.

Bulger, M., 2005. Hyperacetylated chromatin domains: lessons from heterochromatin. J. Biol. Chem. 280, 21689–21692.

Calzone, F.J., Britten, R.J., Davidson, E.H., 1987. Mapping of gene transcripts by nuclease protection assays and cDNA primer extension. Methods Enzymol. 152, 611–632.

Chodosh, L.A., Baldwin, A.S., Carthew, R.W., Sharp, P.A., 1988. Human CCAAT-binding proteins have heterologous subunits. Cell 53, 11–24.

Chomczynski, P., Sacchi, N., 1987. Single-step method of RNA isolation by acid guanidinium thiocyanate-phenol-chloroform extraction. Analyt. Biochem. 162, 156–159.

Corden, J., Wasylyk, B., Buchwalder, A., Sassone-Corsi, P., Kedinger, C., Chambon, P., 1980. Promoter sequences of eukaryotic protein-coding genes. Science 209, 1406–1414.

Dignam, J.D., Lebovitz, R.M., Roeder, R.G., 1983. Accurate transcription initiation by RNA polymerase II in a soluble extract from isolated mammalian nuclei. Nucleic Acids Res. 11, 1475–1489.
Dynan, W.S., Tjian, R., 1983. The promoter-specific transcription factor Sp1 binds to upstream sequences in the SV40 early promoter. Cell 35, 79–87.
Fourel, G., Lebrun, E., Gilson, E., 2002. Protosilencers as building blocks for heterochromatin. Bioessays 24, 828–835.
Gustincich, S., et al., 2006. The complexity of the mammalian transcriptome. J. Physiol. 575, 321–332.
Henikoff, S., 1984. Unidirectional digestion with exonuclease III creates targeted breakpoints for DNA sequencing. Gene 28, 351–359.
Hennighausen, L., Lubon, H., 1987. Interaction of protein with DNA in vitro. Methods Enzymol. 152, 721–735.
Hibino, Y., et al., 2006. Molecular properties and intracellular localization of rat nuclear scaffold protein P130. Biochim. Biophys. Acta 1759, 195–207.
Hiraga, K., Kikuchi, G., 1980a. The mitochondrial glycine cleavage system: purification and properties of glycine decarboxylase from chicken liver mitochondria. J. Biol. Chem. 255, 11664–11670.
Hiraga, K., Kikuchi, G., 1980b. The mitochondrial glycine cleavage system: functional association of glycine decarboxylase and aminomethyl carrier protein. J. Biol. Chem. 255, 11671–11676.
Hong, S.-P., Piper, M.D., Sinclair, D.A., Dawes, I.W., 1999. Control of expression of one-carbon metabolism genes of *Saccharomyces cerevisiae* is mediated by a tetrahydrofolate-responsive protein binding to a glycine regulatory region including a core 5′-CTTCTT-3′ motif. J. Biol. Chem. 274, 10523–10532.
Isobe, M., Koyata, H., Sakakibara, T., Momoi-Isobe, K., Hiraga, K., 1994. Assignment of the true and processed genes for human glycine decarboxylase to 9p23–24 and 4q12. Biochem. Biophys. Res. Commun. 203, 1483–1487.
Kanno, J., et al., 2007. Genomic deletion within GLDC is a major cause of non-ketotic hyperglycinemia. J. Med. Genet. 44, e69.
Kawaguchi, T., Nomura, K., Hirayama, Y., Kitagawa, T., 1987. Establishment and characterization of a chicken hepatocellular carcinoma cell line, LMH. Cancer Res. 47, 4460–4464.
Kikuchi, G., 1973. The glycine cleavage system: composition, reaction mechanism, and physiological significance. Mol. Cell. Biochem. 1, 169–187.
Kikuchi, G., Hiraga, K., 1982. The mitochondrial glycine cleavage system: unique features of the glycine decarboxylation. Mol. Cell. Biochem. 45, 137–149.
Kikuchi, G., Motokawa, Y., Yoshida, T., Hiraga, K., 2008. The glycine cleavage system: reaction mechanism, physiological significance, nonketotic hyperglycinemia. Proc. Japan Acad. Ser. B. 84, 246–262.
Kim, J., Kollhoff, A., Bergmann, A., Stubbs, L., 2003. Methylation-sensitive binding of transcription factor YY1 to an insulator sequence within the paternally expressed imprinted gene, Peg3. Hum. Mol. Genet. 12, 233–245.
Kim, M.Y., Zhang, T., Kraus, W.L., 2005. Poly(ADP-ribosyl)ation by PARP-1: 'PAR-laying' NAD^+ into a nuclear signal. Genes Dev. 19, 1951–1967.
Klose, R.J., Bird, A.P., 2006. Genomic DNA methylation: the mark and its mediators. Trends Biochem. Sci. 31, 89–97.
Kume, A., Kure, S., Tada, K., Hiraga, K., 1988. The impaired expression of glycine decarboxylase in patients with hyperglycinemias. Biochem. Biophys. Res. Commun. 154, 292–297.
Kume, A., Koyata, H., Sakakibara, T., Ishiguro, Y., Kure, S., Hiraga, K., 1991. The glycine cleavage system: molecular cloning of the chicken and human glycine decarboxylase cDNAs and some characteristics involved in the deduced protein structures. J. Biol. Chem. 266, 3323–3329.
Kure, S., Koyata, H., Kume, A., Ishiguro, Y., Hiraga, K., 1991a. The glycine cleavage system: the coupled expression of the glycine decarboxylase gene and the H-protein gene in the chicken. J. Biol. Chem. 266, 3330–3334.
Kure, S., Narisawa, K., Tada, K., 1991b. Structural and expression analyses of normal and mutant mRNA encoding glycine decarboxylase: three-base deletion in mRNA causes nonketotic hyperglycinemia. Biochem. Biophys. Res. Commun. 174, 1176–1182.
Kure, S., et al., 2006. Comprehensive mutation analysis of GLDC, AMT, and GCSH in nonketotic hyperglycinemia. Hum. Mutat. 27, 343–352.
Lim, C.L., Fang, L., Swendeman, S.L., Sheffery, M., 1993. Characterization of the molecularly cloned murine α-globin transcription factor CP2. J. Biol. Chem. 268, 18008–18017.
Maniatis, T., Goodbourn, S., Fischer, J.A., 1987. Regulation of inducible and tissue-specific gene expression. Science 236, 1237–1245.
Mantovani, R., et al., 1992. Monoclonal antibodies to NF-Y define its function in MHC class II and albumin gene transcription. EMBO J. 11, 3315–3322.
Matsui, C., Koyata, H., Hiraga, K., 1993. The development-associated increase in the hepatic levels of the intrinsic components of the chicken glycine cleavage system. Arch. Biochem. Biophys. 300, 69–74.
Murata, T., Nitta, M., Yasuda, K., 1998. Transcription factor CP2 is essential for lens-specific expression of the chicken αA-crystallin gene. Genes Cells 3, 443–457.
Nakai, T., Nakagawa, N., Maoka, N., Masui, R., Kuramitsu, S., Kamiya, N., 2005. Structure of P-protein of the glycine cleavage system: implications for nonketotic hyperglycinemia. EMBO J. 24, 1523–1536.
Nathan, D., Sterner, D.E., Berger, S.L., 2003. Histone modifications: now summoning sumoylation. Proc. Natl. Acad. Sci. U.S.A. 100, 13118–13120.
Nyhan, W.L., 1989. Nonketotic hyperglycinemia, In: Scriver, C.R., Beaudet, M.D., Sly, W.S., Valle, D. (Eds.), The Metabolic Basis of Inherited Disease, 6th Ed. McGraw-Hill Information Services Co., New York, pp. 743–753.
Okamura-Ikeda, K., Ohmura, Y., Fujiwara, K., Motokawa, Y., 1993. Cloning and nucleotide sequence of the *gcv* operon encoding the *Escherichia coli* glycine-cleavage system. Eur. J. Biochem. 216, 539–548.
Pantazis, P., West, M.H., Bonner, W.M., 1984. Phosphorylation of histones in cells treated with hypertonic and acidic media. Mol. Cell. Biol. 4, 1186–1188.
Pazin, M.J., Kadonaga, J.T., 1997. What's up and down with histone deacetylation and transcription? Cell 89, 325–328.
Sakakibara, T., et al., 1990. One of the two genomic copies of the glycine decarboxylase cDNA has been deleted at a 5′ region in a patient with nonketotic hyperglycinemia. Biochem. Biophys. Res. Commun. 173, 801–806.
Seglen, P.O., 1976. Preparation of isolated rat liver cells. Methods Cell Biol. 13, 29–34.
Shirra, M.K., Hansen, U., 1998. LSF and NTF-1 share a conserved DNA recognition motif yet require different oligomerization states to form a stable protein–DNA complex. J. Biol. Chem. 273, 19260–19268.
Sinclair, D.A., Hong, S.-P., Dawes, I.W., 1996. Specific induction by glycine of the gene for the P-subunit of glycine decarboxylase from *Saccharomyces cerevisiae*. Mol. Microbiol. 19, 611–623.
Smale, S.T., Baltimore, D., 1989. The "initiator" as a transcription control element. Cell 57, 103–113.
Struhl, K., 1998. Histone acetylation and transcriptional regulatory mechanisms. Genes Dev. 12, 599–606.
Tachibana, M., et al., 2002. G9a histone methyltransferase plays a dominant role in euchromatic histone H3 lysine 9 methylation and is essential for early embryogenesis. Genes Dev. 16, 1779–1791.
Takayanagi, M., et al., 2000. Human glycine decarboxylase gene (GLDC) and its highly conserved processed pseudogene (psiGLDC): their structure and expression, and the identification of a large deletion in a family with nonketotic hyperglycinemia. Human. Genet. 106, 298–305.
van Huijsduijnen, R.H., Li, X.Y., Black, D., Matthes, H., Benoist, C., Mathis, D., 1990. Co-evolution from yeast to mouse: cDNA cloning of the two NF-Y (CP-1/CBF) subunits. EMBO J. 9, 3119–3127.
Venkatesan, K., MacManus, H.R., Mello, C.C., Smith, T.F., Hansen, U., 2003. Functional conservation between members of an ancient duplicated transcription factor family, LSF/Grainyhead. Nucleic Acids Res. 31, 4304–4316.
Walters, M., Kim, C., Gelinas, R., 1991. Characterization of a DNA binding activity in DNAse I hypersensitive site 4 of the human globin locus control region. Nucleic Acids Res. 19, 5385–5393.
Weber, M., et al., 2007. Distribution, silencing potential and evolutionary impact of promoter DNA methylation in the human genome. Nat. Genet. 39, 457–466.
West, A.G., Gaszner, M., Felsenfeld, G., 2002. Insulators: many functions, many mechanisms. Genes Dev. 16, 271–288.
Wilson, R.L., Stauffer, G.V., 1994. DNA sequence and characterization of GcvA, a LysR family regulatory protein for the *Escherichia coli* glycine cleavage enzyme system. J. Bacteriol. 176, 2862–2868.
Wilson, R.L., Steiert, P.S., Stauffer, G.V., 1993. Positive regulation of the *Escherichia coli* glycine cleavage enzyme system. J. Bacteriol. 175, 902–904.
Yamamoto, M., Koyata, H., Matsui, C., Hiraga, K., 1991. The glycine cleavage system: occurrence of two types of chicken H-protein mRNAs presumably formed by the alternative use of the polyadenylation consensus sequences in a single exon. J. Biol. Chem. 266, 3317–3322.

THE JOURNAL OF GENE MEDICINE
J Gene Med 2009; 11: 373–381.
Published online 9 March 2009 in Wiley InterScience (www.interscience.wiley.com) DOI: 10.1002/jgm.1313

RESEARCH ARTICLE

Retroviral vector-producing mesenchymal stem cells for targeted suicide cancer gene therapy

Ryosuke Uchibori[1]
Takashi Okada[1†]
Takayuki Ito[1]
Masashi Urabe[1]
Hiroaki Mizukami[1]
Akihiro Kume[1]
Keiya Ozawa*[1]

[1]*Division of Genetic Therapeutics, Center for Molecular Medicine, Jichi Medical University, Tochigi, Japan*

*Correspondence to: Keiya Ozawa, Division of Genetic Therapeutics, Jichi Medical University, 3311-1 Yakushiji, Shimotsuke, Tochigi 329-0498, Japan.
E-mail: titou@jichi.ac.jp

[†]Present address: Department of Molecular Therapy, National Institute of Neuroscience, National Center of Neurology and Psychiatry, Tokyo, Japan.

Received: 30 May 2008
Revised: 31 October 2008
Accepted: 19 January 2009

Abstract

Background Mesenchymal stem cells (MSCs) are a promising vehicle for targeted cancer gene therapy because of their potential of tumor tropism. For efficient therapeutic application, we developed retroviral vector-producing MSCs that enhance tumor transduction via progeny vector production.

Methods Rat bone marrow-derived MSCs were nucleofected with the proviral plasmids (vesicular stomatitis virus-G protein-pseudotyped retroviral vector components) (VP-MSCs) or pLTR plasmid alone (non-VP-MSCs). The luciferase-based *in vivo* imaging system was used to assess gene expression periodically. To evaluate the anticancer effects, we administered MSCs expressing herpes simplex virus-thymidine kinase (HSV-*tk*) into the left ventricular cavity of nude mice engrafted with 9L glioma cells subcutaneously.

Results *In vivo* imaging revealed that administration of luciferase-expressing non-VP-MSCs enhanced the bioluminescence signal at the inoculation sites of 9L cells, whereas no accumulation was observed in mice at the site of the control Rat-1 fibroblasts. Compared to non-VP-MSCs, the administration of VP-MSCs resulted in significant augmentation of the signal with an increase in transgene copy number. Immunohistochemical analysis showed marked luciferase expression at the tumor periphery in mice injected with VP-MSCs, whereas little expression was detected in those injected with non-VP-MSCs. Under the continuous infusion of ganciclovir, systemic administration of VP-MSCs expressing HSV-*tk* suppressed tumor growth more effectively than non-VP-MSC administration, whereas no anticancer effect was observed without ganciclovir treatment. Furthermore, VP-MSC administration caused no transgene transduction in the normal tissues and organs.

Conclusions VP-MSCs accumulated at the site of tumors after intravascular injection in tumor-bearing mice, followed by *in situ* gene transfer to tumors without transduction of normal organs. When applied to the HSV-*tk*/ganciclovir suicide gene therapy, more efficient tumor growth suppression was observed using VP-MSCs compared to non-VP-MSCs. This VP-MSC-based system has great potential for improved cancer gene therapy. Copyright © 2009 John Wiley & Sons, Ltd.

Keywords HSV-*tk*; in vivo imaging; retroviral vector; suicide cancer gene therapy; vector-producing MSCs

Introduction

Tumor invasions and metastases are the principal causes of death in patients with cancer. However, current anticancer strategies are typically associated with high toxicity and modest success rates. Suicide gene therapy has been tested for the treatment of invasive tumors such as malignant glioma; for this